Characterisation of *Drosophila tipE* as a functional orthologue of the voltage gated Na^+ channel β1 subunit

Lauren Amelia Blackburn (BSc)

MSc by Research

University of York

Biology

December 2018

Abstract

Voltage gated Na^+ channels (VGSCs) are heteromeric protein complexes responsible for the initiation and propagation of action potentials. They consist of pore forming α subunits (Nav1.1 – Nav1.9) and auxiliary β subunits (β1- β4), which modulate channel activity and are cell adhesion molecules. The β1 subunit regulates cell adhesion, neurite outgrowth and neuronal migration. *Drosophila melanogaster* possess many orthologous genes associated with human disease. *Drosophila Temperature Induced Paralysis Locus E* (*tipE*) is considered an auxiliary VGSC subunit due to its ability to increase functional VGSC expression in *Xenopus* oocytes, although unlike β1 it is not thought to regulate adhesion. The *Drosophila* stock *tipE^1,se* carries a point mutation at the *tipE* locus which results in a reversible, temperature-sensitive paralytic phenotype. The purpose of this study was to interrogate the functional effects of β1 and *tipE* expression on physiological behaviour in *Drosophila,* thus ascertaining whether *tipE* may be a functional orthologue to the mammalian VGSC β1 subunit. Through physiological assays, we found a locomotor deficit in both *tipE^1,se* mutant adults and larvae, which is exacerbated by an increase in temperature. Furthermore, we saw an evident trend towards decreased ERG amplitude at elevated temperatures in *tipE^1,se* mutants. Knocking down *tipE* using RNAi and RNAi-dicer2 in various tissues suggested an increased climbing ability and hyperactivity at room temperature in adult *Drosophila*. In contrast, RNAi-dicer2 expressing flies did not show a temperature-sensitive phenotype. Expression of mammalian β1 subunit in the motor neurons of *Drosophila* larvae mildly inhibited larval locomotor function. The work described in this thesis adds new information on *tipE* and β1 function. Our results provide evidence that the *tipE^1,se* mutation may disrupt motor function due to a protein truncation. However, further work is still required to address whether *tipE* can recapitulate β1 function.

List of Contents

List of Tables

List of Figures

Acknowledgements

First of all I would like to express my very great appreciation to my supervisors Dr. William Brackenbury and Dr. Sean Sweeney for their incredible support and encouragement throughout my Masters. Their willingness to give up their time in order to share valuable advice is something I am immensely grateful for. My sincere thanks are also extended to my TAP members Dr. Christoph Baumann and Dr. Chris Elliott for their guidance, in particular to Dr. Chris Elliott for his reassurance and patience with my ERGs. I could not have done it without you!

I would also like to thank all members of the Brackenbury and Sweeney labs, both past and present. In particular Faheem Patel, who took me under his wing during the first weeks of my Masters and Alex Haworth, whose assistance and knowledge, especially mathematical, was invaluable (even if you do have a terrible taste in radio station). Thanks to Tess Lesley for always putting a smile on my face in the lab and to Andy James for sharing your insane GraphPad knowledge!

Finally, I would like to thank my parents, who have unconditionally supported me throughout, and especially my brother Harry who swiftly jumped in to solve my last minute “lost work” trauma. In addition, I would like to thank my boyfriend Joel who has no doubt prevented many more traumas with his endless encouragement and optimism.

It has not been an easy 2 years but I am eternally grateful for the opportunity and would do it all again in a heartbeat.

Author’s Declaration

I declare that this thesis is a presentation of original work and I am the sole author. This work has not previously been presented for an award at the University of York, or any other University. All sources are acknowledged as References.

1. Introduction

1.1. A brief overview

Voltage gated Na^+ channels (VGSCs) are heteromeric protein complexes responsible for the initiation and propagation of action potentials (Naylor *et al.*, 2016). They consist of pore forming α subunits ($Na_v1.1$ – $Na_v1.9$) and smaller auxiliary β subunits (β1- β4), which modulate channel activity and are cell adhesion molecules (O'Malley & Isom, 2015). The β1 subunit, encoded by the *SCN1B* gene, regulates cell adhesion, neurite outgrowth and neuronal migration amongst other functions (O'Malley & Isom, 2015). Mutations in *SCN1B* have been found to cause various cardiac and neuronal diseases in humans such as epilepsy, cancer, arrhythmia and neurodegenerative disorders (Wallace *et al.*, 1998; Chen *et al.*, 2004; Brackenbury *et al.*, 2008; Diss *et al.*, 2008; Chioni *et al.*, 2009; O'Malley & Isom, 2015). *Drosophila melanogaster* is a widely used model organism employed to model a variety of human pathologies ranging from Alzheimer's disease and Parkinson's disease to genetic studies into postnatal cardiac function, wound healing and drug discovery. Interestingly, no β subunit orthologues have been discovered in *Drosophila,* however research has suggested that *Temperature induced paralytic locus E* (*tipE*), a novel, integral membrane protein on chromosome III is a VGSC auxiliary subunit (Kulkarni & Padhye, 1982; Warmke *et al.*, 1997; Littleton & Ganetzky, 2000; Hodges *et al.*, 2002). Thus, *tipE* may be a functional orthologue to the mammalian VGSC β1 subunit. Much remains to be understood about the protein and its roles and functions within the *Drosophila* nervous system. With the use of the advanced genetics, locomotor assays, electrophysiology and confocal microscopy, the aim of this project was to better understand the

function and localisation of *tipE* in order to determine whether or not it can be classed as a functional orthologue of mammalian β1.

1.2. Voltage-gated sodium channels

Voltage-gated Na^+ channels (VGSCs) are integral transmembrane glycoproteins responsible for the initiation and propagation of action potentials, facilitating electrical signalling across cellular membranes (Naylor *et al.*, 2016). When a stimulus triggers depolarisation of the plasma membrane, VGSCs open causing an influx of Na^+ into the cell, down an electrochemical gradient. This influx ultimately results in further VGSCs opening, as a result of further membrane depolarisation towards the equilibrium potential for Na^+ (~+60 mV in most neurons) (Eijkelkamp *et al.*, 2012). This process, known as channel activation, causes the rapid rising phase of action potentials. Within milliseconds (ms), VGSCs rapidly inactivate in a process called fast inactivation, which results in the termination of action potentials, allowing an efflux of potassium (K^+) through voltage-gated K^+ channels to return the membrane to its resting potential. VGSCs then enter a process called slow inactivation, which regulates membrane excitability, action potential patterns and spike frequency adaptations (Hsu *et al.*, 2017).

Mammalian neuronal VGSC complexes consist of a single α subunit and two β subunits (Figure 1.1). The former are pore forming, occupying four repeat homologous domains (DI-DIV), each with six membrane spanning segments (S1-S6) and facilitate Na^+ transport across the plasma membrane (Brackenbury & Isom, 2011). These segments consist of a voltage-sensing domain (VSD; S1-S4) in which the highly conserved S4 segment acts as the voltage sensor. The

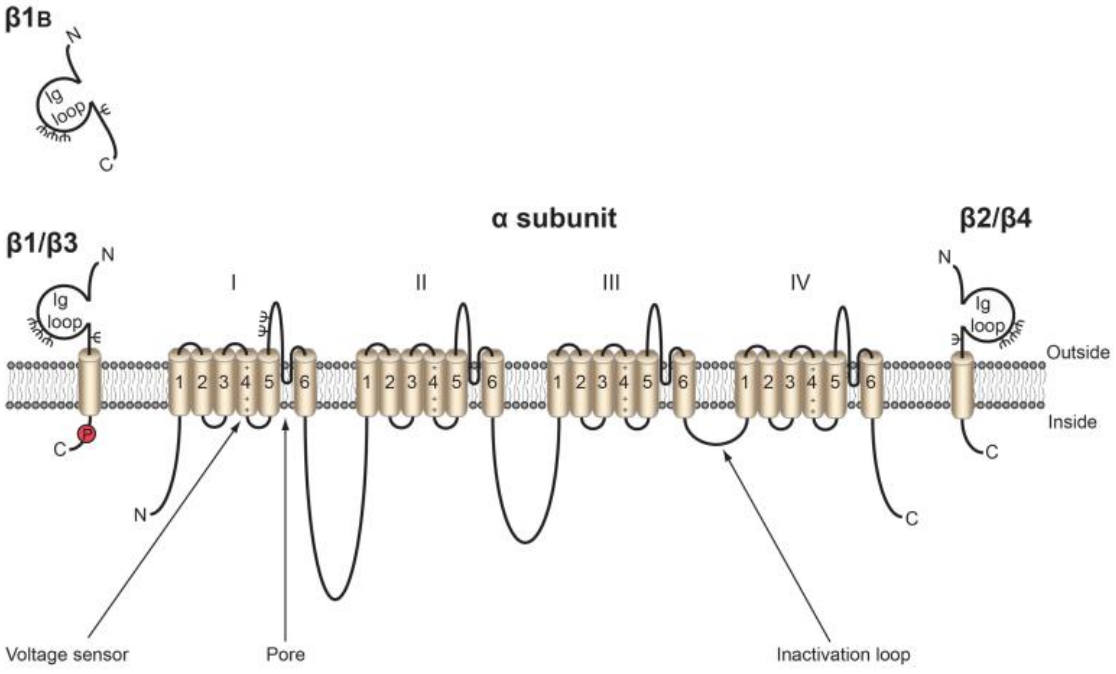

Figure 1.1 VGSC α and β subunit topology. There are nine pore-forming mammalian α subunits ($Na_v1.1$-$Na_v1.9$) encoded by nine distinct genes. Four repeat homologous domains are present, each with six membrane spanning-segments. β subunits consist of a single transmembrane domain, an extracellular N-terminal region with an immunoglobulin loop and an intracellular C-terminal domain. (Adapted from Brackenbury & Isom, 2011)

voltage sensitivity of the S4 segment is due to positively charged amino acid residues along its helix (Ahern *et al.*, 2016). There are nine mammalian VGSC α subunits, named $Na_v1.1$-$Na_v1.9$, which are encoded by nine distinct genes (Table 1.1) (Patel & Brackenbury, 2015; Roger *et al.*, 2015). Each α subunit protein is approximately 260 kDa. In addition, a non-voltage sensitive subtype, Na_x, has been identified. Na_x is believed to regulate Na^+ concentration in order to maintain body fluid homeostasis (Bagal *et al.*, 2015). Four individual genes, *SCN1B*-*SCN4B*, encode five β subunits: β1-β4 and β1B, an alternative splice variant of β1. With the exception of β1B, β subunits consist of a single transmembrane domain, an extracellular N-terminal region with an immunoglobulin (Ig) loop and a smaller intracellular C-terminal region. β1 and β3 are linked to the α subunit by non-covalent bonds, in contrast to the covalent disulphide bonds that link β2 and β4 to the α subunit (Patel & Brackenbury, 2015). β subunits have multiple conducting and non-conducting roles such as regulation of channel expression and gating, as well as participating in *trans*-homophilic adhesion. This adhesion results in cellular aggregation and recruitment of the cytosolic protein Ankyrin-G to points of cell-cell contact. β subunits are therefore members of the Ig superfamily of cell adhesion molecules (CAMs) (Isom *et al.*, 1995; Malhotra *et al.*, 2000; Yu *et al.*, 2003).

1.3. β1 subunit

Encoded by the gene *SCN1B,* the β1 transcript is spliced from exons 1-5, unlike the β1B splice variant, which is spliced from exons 1-3 (Watanabe *et al.*, 2008). The β1 subunit works in concert with the α subunit to promote channel trafficking to the plasma membrane (O'Malley & Isom, 2015). It regulates cell

Table 1.1: Expression and localisation of mammalian VGSC α subunits.

Gene[1]	*α subunit encoded*	*Tissue localisation*
SCN1A	$Na_v1.1$	CNS, PNS, heart
SCN2A	$Na_v1.2$	CNS, PNS
SCN3A	$Na_v1.3$	CNS, PNS
SCN4A	$Na_v1.4$	Skeletal muscle
SCN5A	$Na_v1.5$	Uninnervated skeletal muscle, heart, brain
SCN8A	$Na_v1.6$	CNS, PNS, heart
SCN9A	$Na_v1.7$	PNS, sensory neurons
SCN10A	$Na_v1.8$	Sensory neurons
SCN11A	$Na_v1.9$	Sensory neurons

[1]Adapted from Patel & Brackenbury, 2015; Roger *et al,* 2015.

adhesion, neurite outgrowth and neuronal migration, as well as playing a critical role in axon pathfinding and fasciculation during early central nervous system (CNS) development (Brackenbury *et al.*, 2008; Patel & Brackenbury, 2015). The expression profile of β1 is diverse within the vertebrate nervous system and cardiac tissues (Table 1.2) and has been found to predominate in post-natal development (O'Malley & Isom, 2015). Mutations in *SCN1B* have been found to cause various cardiac and neuronal diseases in humans including epilepsy and cardiac arrhythmia (Wallace *et al.*, 1998; Chen *et al.*, 2004; Brackenbury *et al.*, 2008; Diss *et al.*, 2008; Chioni *et al.*, 2009; O'Malley & Isom, 2015). Similarly, *SCN1B* null mice exhibit ataxia, spontaneous seizures and a prolonged cardiac QT interval (Chen *et al.*, 2004; Lopez-Santiago *et al.*, 2007).

1.4. *Drosophila* as a model organism

Drosophila melanogaster is a widely used model organism employed to investigate a variety of human diseases and has been studied in detail for over a century. A complex multicellular organism, it has been used in the research of many human pathologies ranging from neurodegenerative diseases such as Alzheimer's disease and Parkinson's disease to genetic studies into postnatal cardiac function, wound healing and drug discovery (Wolf & Rockman, 2008; Jennings, 2011; Prüßing *et al.*, 2013). The small size, short generation time, uncomplicated diet and advanced genetic toolbox are just some of the advantages of working with *Drosophila*. A poikilothermic animal, which is viable over a range of temperatures, *Drosophil*a are often reared at 18 °C to 25 °C.

Drosophila possess four pairs of chromosomes: an XX/XY pair and 3 autosomal pairs. There are approximately 14,000 genes within the *Drosophila* genome,

Table 1.2: Tissue specific expression profile of β1.

Location in nervous system[1]	***Reference***
Hippocampal neurons	(Chen *et al.*, 2004)
Cortical neurons	(Nguyen *et al.*, 2012)
Purkinje neurons	(Brackenbury *et al.*, 2010)
Cerebellar granule neurons	(Davis *et al.*, 2004; Brackenbury *et al.*, 2010)
Astrocytes	(Oh *et al.*, 1997; Aronica *et al.*, 2003; Cahoy *et al.*, 2008)
Bergmann glia	(Davis *et al.*, 2004)
Nodes of Ranvier	(Ratcliffe *et al.*, 2001; Chen *et al.*, 2004)
Dorsal root ganglia	(Oh *et al.*, 1995; Lopez-Santiago *et al.*, 2006; Zhao *et al.*, 2011)
Location in cardiac tissues	
Ventricular myocytes	(Maier *et al.*, 2004)
Atrial myocytes	(Gaborit *et al.*, 2007; Kaufmann *et al.*, 2013)
Sino-atrial node	(Maier *et al.*, 2003)

[1]Adapted from O'Malley and Isom, 2015.

with around 75% of genes known to cause disease in humans having a *Drosophila* equivalent (Jennings, 2011). Compared to the human genome, there is a reduced genetic redundancy in the genome of *Drosophila*. This has enabled study of many signalling and developmental processes, leading to the discovery of numerous genes contributing to tumorigenesis and nervous system function when either mutated or dysregulated. For example, abnormal expression of *Drosophila* neoplastic tumour suppressors, such as the apical-basal cell polarity regulators within the hippo pathway, have been associated with differentiation abnormalities and over-proliferation as a result of failing to exit the cell cycle (Chen *et al.*, 2010).

1.5. The UAS-GAL4 bipartite system in *Drosophila* genetics

The UAS-GAL4 system is a bipartite ectopic expression system carried in separate genetic stocks of *Drosophila*, enabling the effects of expression of single transgenes in different tissues or at different stages of development to be analysed (Figure 1.2) (Duffy, 2002). The upstream activation sequence (UAS), present in the responder line, is a non-coding DNA region that regulates nearby gene transcription, ultimately increasing expression. GAL4, present in the driver line and expressed via a promoter of choice, encodes a yeast transcription activator protein. When the two stocks are crossed and both constructs are inherited by the offspring, GAL4 binds to the UAS region, activating transcription of a reporter gene downstream. Importantly, GAL4 is not endogenously expressed in *Drosophila*, and without it, responder transcription maintains a transcriptionally silent state (Duffy, 2002). *P*-element transposon based vectors are used to integrate exogenous GAL4 into the *Drosophila* genome (Brand & Perrimon, 1993.; Duffy, 2002; Baker *et al.*, 2007).

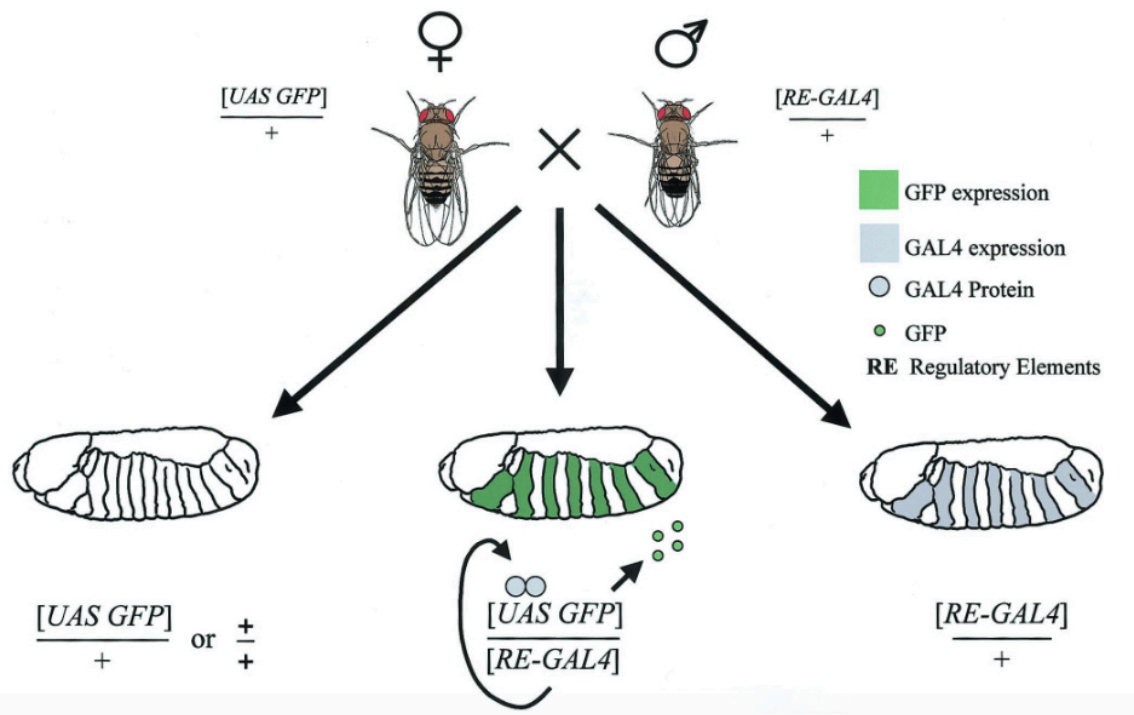

Figure 1.2. The UAS-GAL4 bipartite system. Fly stocks carrying a UAS responder, for example UAS-GFP, are crossed to a different stock carrying a GAL4 driver. As a result, progeny produced from the above cross contain both elements of the UAS-GAL4 system. The presence of GAL4 in the banded segmental pattern in the embryos drives the expression of UAS-GFP in a corresponding pattern. (Adapted from Duffy, 2002).

1.6. The *Drosophila* nervous system

Drosophila provide a valuable paradigm for studying both morphology and function of the nervous system. This is due to the highly established, clonal system of development that allows for genetic manipulation within a manageable number of neurons. Within the *Drosophila* brain, groups of neurons that have derived from a single "parent" neuroblast are assembled into approximately 100 clonal units called lineages, which project in a unified direction (Spindler & Hartenstein, 2010). This combination of many neurons into a single lineage means the magnitude is dramatically increased, allowing for cellular level analysis to be carried out at a much more practicable resolution. These lineages can easily be visualized using both antibodies and GAL4 constructs which allows for areas of neuronal development, such as branch formation, circuit formation and axon guidance, to be studied (Spindler & Hartenstein, 2010; Kremer *et al.*, 2017). The typical size of an adult *Drosophila* brain is 590 μm × 340 μm × 120 μm (Peng *et al.*, 2011). The average early first instar larval brain has a diameter of approximately 50 μm, consisting of 1500 differentiated functional nerve cells (Cardona *et al.*, 2009; Larsen *et al.*, 2009). In addition to this, *Drosophila* synaptic proteins have been found to be, on average, over 70% similar to those found in mammalian systems and, with a small number of exceptions, the majority of mammalian proteins have a *Drosophila* orthologue (Frank *et al.*, 2013).

As a model synapse, the *Drosophila* larval neuromuscular junction (NMJ) exhibits an archetypal structure with clearly distinguishable components both pre and postsynaptically that can easily be compared between genotypes (West *et al.*, 2015*a*). The well-characterised and amenable glutamatergic synapse is

consistent in size and connectivity between larvae and is thus a highly effective tool for the study of neurotransmission and synaptic development. This level of consistency is not possible with the vertebrate CNS, however the structural and functional similarity between the two allows for a robust comparison to be made (Koh *et al.*, 2000; West *et al.*, 2015*a*). The NMJs most commonly studied in *Drosophila* are the ventral longitudinal abdominal muscle fibres m6 and m7 (Crossley *et al.*, 1978). Two distinct axons contribute to the innervation of the above NMJ, axons I and II. The former provides approximately 800 synaptic release sites to m6 and m7, and the latter approximately 250 synaptic release sites (Atwood *et al.*, 1993).

1.7. *Drosophila* Na^+ channels

Drosophila possess a single VGSC gene, which is X-Linked (Kroll *et al.*, 2015). $DmNa_V$ is a large gene, spanning approximately 60 kb of genomic DNA and encodes the equivalent of the mammalian VGSC α subunit (Kroll *et al.*, 2015). Formerly known as *para*, the single gene is able to encode multiple variants of the protein as a result of extensive alternative splicing, RNA editing and post-transcriptional modification (Lin *et al.*, 2009). In addition to $DmNa_V$, *Drosophila Sodium Channel 1* (*DSC1*) encodes a VGSC-like cation channel. Despite *DSC1* having a high sequence similarity to the transmembrane regions of VGSCs, it has been found to have a higher permeability to Ca^{2+} as opposed to Na^+ (Dong *et al.*, 2015). Although *DSC1* does not encode a functional Na^+ channel in itself, gene knockout has shown alterations in *Drosophila* behaviour and neuronal physiology, especially after heat shock or starvation, suggesting the DSC1 channel plays a role in modulating neuronal circuit stability. This is likely achieved by maintaining the sustainability of synaptic transmission (Zhang *et*

al., 2013; Rinkevich *et al.*, 2015). Importantly, no β subunit orthologues have been discovered in *Drosophila*, suggesting that such subunits are a result of an evolution event after the arrival of invertebrates (Littleton & Ganetzky, 2000).

1.8. The *Drosophila tipE* locus encodes an auxiliary VGSC subunit

Temperature sensitive paralytic mutations were first described in the early 1970's by Suzuki and his colleagues (Suzuki *et al.*, 1971). In the early 1980's, 4544 lines of *Drosophila* autosomes were treated with ethylmethanesulphonate (EMS), a mutagen that produces random mutations, typically point mutations, in genetic material by nucleotide substitution. From the mutations generated, seven temperature sensitive paralytic mutants were recovered and given the name "temperature-induced paralytic" (tip). The tip mutations belong to six different genes: *tipA*, *TipB*, *tipC* and *tipD* on the second chromosome, with *tipE* and *tipF* on the third chromosome (Kulkarni & Padhye, 1982).

There are four genetic loci within the *Drosophila* genome that are known to affect the structure or function of VGSCs. These loci include *temperature-sensitive paralysis* (*para*), *temperature-sensitive no action potential* (*nap*), *temperature-sensitive seizure* (*sei*) and *temperature-induced paralytic locus E* (*tipE*) (Feng *et al.*, 1995*a*). *tipE* encodes a novel, integral membrane protein, located at cytogenetic position 64A10 on chromosome III that is a VGSC auxiliary subunit within *Drosophila* (Kulkarni & Padhye, 1982). *tipE* possesses two transmembrane domains, as opposed to the one seen in the mammalian β subunit, with both the N-terminus and C-terminus of the protein being located intracellularly. Five possible glycosylation sites have been predicted (Figure 1.3)

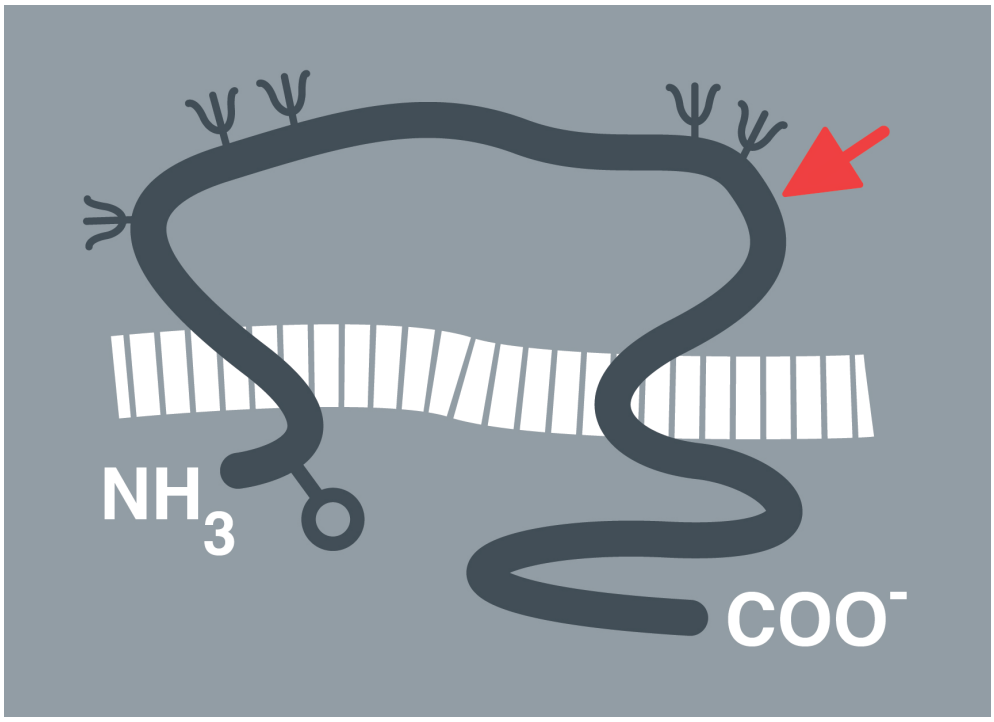

Figure 1.3. Predicted membrane topology of *tipE*. The arrow indicates the approximate location of the T to A transversion point mutation seen in *tipE* mutants. This occurs at nucleotide position 714, causing a cysteine residue to be changed to a premature STOP codon, potentially resulting in relocation of the C-terminus extracellularly. The open circle indicates a protein kinase C (PKC) phosphorylation site. Psi indicates five predicted N-glycosylation sites (Adapted from Feng *et al*, 1995).

(Feng *et al.*, 1995*a*). Although there is little sequence similarity between *tipE* and any mammalian VGSC proteins, functional expression of *para* Na^+ channels is increased when *tipE* is expressed in *Xenopus laevis* oocytes (Feng *et al.*, 1995*a*). *tipE* does not form a functional VGSC on its own. However when co-expressed in *Xenopus* oocytes with para cRNA, expression of *Drosophila* VGSC α subunits is increased, indicating *tipE* supports the expression of functional VGSCs and modulates channel gating (Warmke *et al.*, 1997; Hodges *et al.*, 2002). Whole mount *in situ* hybridisation of *Drosophila* embryos showed the protein to be strongly expressed in the CNS, but more weakly expressed in the peripheral nervous system (PNS). *tipE* is most highly expressed in the mid to late pupal stages of development (Feng *et al.*, 1995*a*). Additionally, four sequences named TEH1-4 have been described as being homologous to *tipE* within the *Drosophila* genome (Derst *et al.*, 2006). The sequences consist of two transmembrane domains, short cytosolic N and C terminal stretches and a large extracellular loop with two disulphide bonds, which are characteristic of both *tipE* and the β subunit (Sloβ) subunit of large conductance Ca^{2+}-activated potassium (BK) channels. BK channel Sloβ subunits control a large variety of physiological processes, including smooth muscle contraction, neurosecretion, and hearing development (Orio *et al.*, 2002).

The *Drosophila* stock *tipE*^{1},*se* carries a T to A transversion point mutation at nucleotide position 714 which results in a cysteine residue being changed to a premature STOP codon (Feng *et al.*, 1995*a*). These flies show a reversible, temperature sensitive paralytic phenotype at 38 °C (Kulkarni & Padhye, 1982). It is currently unknown if the protein is still present as a result of the nonsense mutation or whether mRNA carrying the premature termination codon is being

degraded by nonsense mediated decay. If the protein is present, it would result in a truncated protein of 237 amino acids with the C terminal region being relocated extracellularly. If the nonsense mediated decay pathway has been activated in order to degrade the mRNA, the mutation could be generating an effective null allele.

1.9. The *Drosophila* visual system

The *Drosophila* visual system and its underlying neuronal mechanisms have facilitated the gathering of critical genetic information on neurological function and continues to contribute greatly to our understanding of higher order brain function (Zhu, 2013). The *Drosophila* visual system consists of two main components: the retina, in which visual information is detected and the optic lobe, in which visual processing occurs (Figure 1.4). The retina, able to detect a range of light from UV to green, comprises 750-800 ommatidia. Each ommatidial unit contains eight photoreceptor neurons (R1-8), which project into the optic lobe. Photoreceptors R1–6 express a rhodopsin most sensitive to blue light. R7 detects UV light whilst R8 detects either blue or green light. It is through structures known as rhabdomeres, where rhodopsin is housed, that light stimuli are received by photoreceptors (Sato *et al.*, 2013).

Visual information received in the retina is transmitted to the optic lobe, which contains two types of neuron: interneurons, in which the cell bodies and projections remain within the optic lobe; and projection neurons, which connect the optic lobe to the central brain (Nériec & Desplan, 2016). The optic lobe can be subdivided into four ganglia: the lamina, medulla, lobula and lobula plate, in which the latter two structures can be collectively known as the lobula complex.

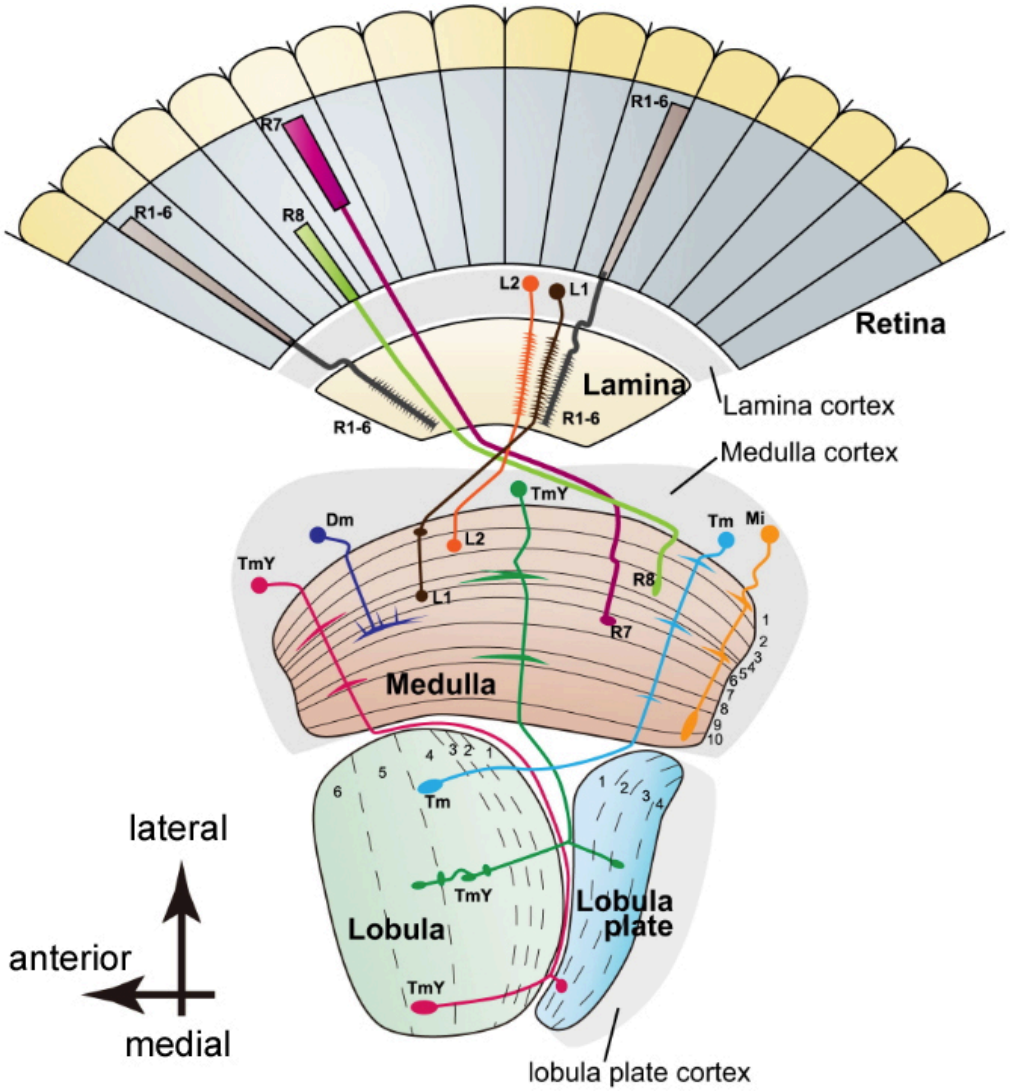

Figure 1.4. Schematic drawing of a horizontal section of the *Drosophila* visual system. The *Drosophila* visual system is made up of the retina, in which visual information is detected and optic lobe, in which visual processing occurs. The latter is subdivided into the lamina, medulla, lobula and lobula plate. The lamina is mostly composed of interneurons, made up of five different types of monopolar neurons and amacrine cells. The structurally layered medulla receives direct innervation from both colour photoreceptors and monopolar neurons in the lamina and ensures accurate visual representation for the fly. The lobula is made up of a majority of projection neurons. The lobula plate neuropil is subdivided into 4 layers and represents the output centre of neural circuits that process motion (Adapted from Sato et al., 2013).

R1-6 axons project into the lamina, whereas R7-8 axons project through the lamina to the medulla. The lamina is mostly composed of interneurons, made up of five different types of monopolar neurons and amacrine cells. The medulla is structured into ten layers (M1-10, M1-6 being known as the distal medulla and M7-10 the proximal medulla) and contains approximately 40,000 interneurons. It receives direct innervation from both colour photoreceptors and monopolar neurons in the lamina and as a whole, ensures accurate visual representation for the fly. The lobula is subdivided into six layers and is made up of a majority of projection neurons. The lobula plate neuropil is subdivided into 4 layers and represents the output centre of neural circuits that process motion (Sato *et al.*, 2013; Nériec & Desplan, 2016).

1.10. The *Drosophila* electroretinogram

The electroretinogram (ERG) allows for the assessment of visual function (Hindle *et al.*, 2013). This is carried out by measuring electrical activity, generated by cells in the retina, in response to a light stimulus. The response occurs following a change in transretinal ions, usually Na^+ and K^+. The *Drosophila* ERG has been used for more than 40 years, allowing for the characterisation of phototransduction (Pak, 2010). It works by recording compound field potentials from photoreceptors and downstream neurons in the fly eye, using an extracellular electrode, in response to flashes of light. Postsynaptic potentials in the visual system neurons cause a transient voltage spike within the ERG trace when the light is both switched on and off. For example, in wildtype flies, the corneal-positive “on” transient is seen within ten milliseconds of the initiation of a light stimulus and corresponds to hyperpolarisation of the laminar neurons (Vilinsky & Johnson, 2012). A corneal-

negative “off” transient is seen within ten ms of the termination of the light stimulus and corresponds to repolarisation of the laminar neurons. The sustained negative receptor potential follows the initial corneal-positive “on” transient and reflects the depolarisation of photoreceptors. On average, within 100 ms of the initial light pulse, the trace reading should reach a maximum of 10-20 mV (Vilinsky & Johnson, 2012). Temperature sensitive paralysis mutants have been reported to have reduced “on” and “off” transient ERG peaks, which eventually disappear altogether, directly correlating to an increase in temperature (Kelly & Suzuki, 1974).

1.11 Hypothesis and aims

The central hypothesis for this project was that *tipE* is a functional orthologue of the VGSC β1 subunit. This is based on the results of previous work carried out on *tipE* and β1 showing that both proteins modulate channel gating and expression in different model systems (Isom *et al.*, 1992; Feng *et al.*, 1995*a*). There were two specific aims:

Aim 1. To investigate the *tipE* mutant phenotype

The goal here was to recapitulate and expand previous analysis of the temperature-sensitive phenotype using temperature shift experiments, paralysis, larval crawling assays and ERGs. To date, the phenotype of $tipE^{1}$,*se* mutants has been examined in homozygosity. In order to exclude the possibility that the *sepia* background could be partially responsible for the phenotypes observed, we examined *tipE* mutants in trans to a genetic deficiency uncovering the region of the *tipE* locus. Experiments were carried out on both $tipE^{1}$,*se*

mutant flies and $+;+;\frac{tipE1,se}{Df(3L)GN50}$ flies at both non-permissive and permissive temperatures. In order to study whether the *tipE* mutation generated a functional null allele, we also compared the phenotype to flies in which *tipE* had been knocked down using RNAi.

Aim 2. To study β1 localisation and functionality within the *Drosophila* larval brain and adult neurons

The hypothesis of this aim was that β1 could recapitulate *tipE* localisation and function in *Drosophila* neurons. We tested this using a previously constructed mammalian β1 transgene. The transgene consists of mammalian β1 fused to the EGFP reporter within the pUASt vector, which was microinjected into *Drosophila.* Expression using the UAS-GAL4 system with a range of neuronal drivers allowed mammalian β1 localisation to be visualised using confocal microscopy. Additionally, the goal was to establish whether the β1 transgene could rescue the *tipE[1],se* mutant phenotype, thus providing a further insight into whether the two could act as functional orthologues.

2. Materials and Methods

2.1. Vectors

Work was carried out by a previous student to create two plasmids: pUAST.*tipE* and pUAST.β1-EGFP. The plasmids were created in order for the *tipE* and mammalian VGSC β1 transgenes to be microinjected into stocks bearing the AttP2 second chromosome landing site. pUAST.*tipE* was created using the pUAST-AttB vector and the pOT2-*tipE* vector. The former is a plasmid designed for generating donor plasmids that can be used to insert sequences containing an open reading frame of interest, expressed under the control of UASt regulatory sequences, into an attP-containing docking site in the genome in *Drosophila* (Bischof *et al.*, 2007). The latter contained the original cDNA encoding the *tipE* open reading frame (ORF) (Brand & Perrimon, 1993; Allaway *et al.*, 2001). pUAST.β1-EGFP was created using the pUAST-AttB vector and the pEGFPN1.β1 vector, which was originally generated by inserting β1 cDNA lacking the stop codon into the pEGFPN1 vector to create a C-terminal fusion protein with EGFP (Chioni *et al.*, 2009).

2.2. Sequencing of pUAST.*tipE* and pUAST.β1-EGFP vectors

pUAST.*tipE* and pUAST.β1-EGFP were made previously by a former student, therefore we first sequenced them to confirm identity. Sequencing primers were designed to complement sequences present within the *tipE* and UAS inserts of the pUAST.*tipE* vector using Primer3 and NCBI Primer-BLAST (Table 2.1). Custom primers were supplied by Sigma-Aldrich, UK with the GATC service used to sequence the pUAST.*tipE* vector. Custom primers supplied by Sigma-Aldrich, UK were used to amplify the β1 sequence, with SourceBioscience, UK stock primers used to amplify the *EGFP* sequence within pUAST.β1-EGFP.

SourceBioscience, UK were used to sequence the pUAST.β1-EGFP vector (Table 2.1). Unfortunately, pUAST.*tipE* was found to contain a STOP codon upstream of *EGFP*. This meant the stocks this vector had already been microinjected into could not be used to visualise *tipE*-GFP expression. In order to be able to select the correct genotype of progeny following a genetic cross, we required the tipE protein to be correctly fused to EGFP to create the fusion protein tipE-EGFP. This would allow us to select GFP+ larvae using a fluorescence microscope.

2.3 DNA extraction

Genomic DNA was extracted from whole *Drosophila* (genotypes: *Canton-S* and *tipE*^{1}*,se*) using a single fly squish protocol based on that published previously (Gloor *et al.*, 1993). 200 µg/ml (10 µl/ml) proteinase K was added to 50 µl squishing buffer (10 mM Tris pH 8.2, 25 mM NaCl, 1 mM EDTA), which was used to homogenise flies. Homogenates were incubated first at 37 °C for 30 minutes, then at 85 °C for 10 minutes and spun down.

2.4 PCR

PCR was carried out on the fly samples and the resulting fragments subjected to sequencing. Reactions contained 10 µl MasterMix (Promega), 2 µl primer mix (10 µl forward primer, 10 µl reverse primer, 80 µl dH_2O), 1 µl sample and 7 µl dH_2O (total = 25 µl reactions). The PCR programme used was as follows: initialisation at 95°C for 5 minutes, followed by 30 cycles of denaturation at 92 °C for 30 seconds, annealing at 60.6 °C for 40 seconds, extension at 72 °C for 90 seconds, with a final extension of 72 °C for 10 minutes. Primers for PCR

Table 2.1 – Sequencing primers

Primer	*Sequence*	*Sequencing Company*
pUAST.tipE		
tipE1-F	5’ - GGGAGACGAGCAGGACAAA	GATC
tipE1-R	5’ - GAAGATCGTGGTGAAGGCG	GATC
tipE2-F	5’ - GGACATCTATACGTGCACCC	GATC
tipE2-R	5’ - GCCTGGCTCCCACATAGTAG	GATC
tipE3-F	5’ - CCCCTGCTACTACTCCAAGG	GATC
tipE3-R	5’ - CGGACTCTGCGCGATGTA	GATC
UAS1-F	5’ - CTTCGTCTACGGAGCGACAA	GATC
UAS1-R	5’ - CTTGTTCAGCTGCGCTTGTT	GATC
UAS2-F	5’ - GCGAGCGCCGGAGTATAAAT	GATC
UAS2-R	5’ - GCGACGTGTTCACTTTGCTT	GATC
pUAST.β1-EGFP		
β1-F	5’ - GTCGTCAAGAAGATCCACATTGAGGT	Source Bioscience, UK
EGFP NRev	5’ - CGTCGCCGTCCAGCTCGACCAG	Source Bioscience, UK

were designed to amplify endogenous *tipE* using NCBI Primer-BLAST and supplied by Sigma-Aldrich. Separate custom primers were created for sequencing, which was carried out by the GATC service (Table 2.2).

2.5. *Drosophila* stocks and maintenance

Drosophila stocks were raised on a standard cornmeal–yeast–sucrose medium at 25°C on a 12 h light:dark cycle. *Canton-S* outcrossed to w^- flies were used as wild type controls (WT), with the exception of those used in the $tipE^1$,*se* paralysis assay which were *Canton-S* and those used in the ERGs which were w^+;+;se^1. The following stocks were used:

I. ***tipE*^{1}*, se* for paralysis assay:** The $tipE^1$,*se* mutant stock was used, with the wild type stock *Canton-S* used as a control. Generally, wild type stocks are outcrossed in order to offset the effects of inbreeding within an older stock. Due to the nature of this experiment, in which the older, inbred $tipE^1$,*se* mutant stock was being analysed without outcrossing, *Canton-S* was also not outcrossed.

II. ***tipE*^{1}*,se and*** $+;+;\frac{tipE^1,se}{Df(3L)GN50}$ **for locomotor and climbing assays:** The $tipE^1$,*se* mutant stock was used, with the outcrossed wild type stock used as a control. $tipE^1$,*se* were crossed to the deficiency stock $+;+;\frac{Df(3L)GN50}{TM8}$, which uncovers the region 63E1-63E2;64B17, in order to create $+;+;\frac{tipE^1,se}{Df(3L)GN50}$. The *TM8* balancer chromosome in $+;+;\frac{Df(3L)GN50}{TM8}$ stocks carries the *stubble* (*sb*) gene as a marker, resulting in shortened, stubbly hairs on the back of the fly. In order to ensure the correct $+;+;\frac{tipE^1,se}{Df(3L)GN50}$ genotype was selected, flies lacking the *sb* marker and consequently the *TM8* balancer were selected.

Table 2.2 – Primers created for amplification and sequencing of endogenous *tipE* from *Drosophila* DNA

Primer	***Sequence***	***Used For***
tipE1-F	5’ - GGGAGACGAGCAGGACAAA	PCR
tipE1se-R	5’ - CTGAATCGGAATCTAACATTTTCCA	PCR
tipE-F-seq	5’ - AGACGAGCAGGACAAAC	Sequencing
tipE-R-seq	5’ – GGAGGAGTTGAGATACTCG	Sequencing

III. $+;+;\frac{\boldsymbol{tipE^1,se}}{\boldsymbol{Df(3L)GN50}}$ **for paralysis assay:** outcrossed WT, *tipE[1],se* mutants and $+;+;\frac{Df(3L)GN50}{TM8}$ were used as controls. *tipE[1],se* mutants were outcrossed to *w[-]* to create $\frac{w^-}{+};+;\frac{tipE^1,se}{+}$ in order to establish if temperature sensitive paralysis was present in heterozygous *tipE[1],se* mutants, in addition to the original homozygous stock. $+;+;\frac{tipE^1,se}{Df(3L)GN50}$ were created as above. *Df(3L)GN50* does not uncover *se.* The *tipE[1]* mutation was induced in an *se* background and study of the *tipE[1]/Df(3L)GN50* transheterozygote will point to any role for se in temperature sensitive paralysis. Homozygous *se* mutants were tested for temperature sensitive paralysis and were found to behave in the manner of a wildtype fly and did not paralyse with increasing temperature (data not shown).

IV. **Stocks for RNA interference:**

- **RNAi alone**: The transgenic RNAi project (TRiP) RNAi stock $+;+;\frac{UAS-tipE-RNAi}{TM3,sb}$ was crossed to a global driver $(+;\frac{Act5C-GAL4}{CyO-GFP};+)$, a pan-neuronal driver $(+;+;\frac{nSyb-GAL4}{CyO-GFP})$ and a motor-neuronal driver $(+;\frac{OK6-GAL4}{CyO-GFP};+)$ in order to knock down *tipE* expression in the respective tissues, creating the genotypes $+;\frac{Act5C-GAL4}{+};\frac{UAS-tipE-RNAi}{+}$, $+;+;\frac{nSyb-GAL4}{UAS-tipE-RNAi}$ and $+;\frac{OK6-GAL4}{+};\frac{UAS-tipE-RNAi}{+}$. The *TM3,sb* balancer chromosome in $+;+;\frac{UAS-tipE-RNAi}{TM3,sb}$ stocks carries the *tubby* (*tb*) gene as a marker, used for larval identification, in addition to *sb*. Drivers carry the balancer chromosome *CyO-GFP*, a gene causing a curly wing

phenotype fused to GFP, the latter of which is used to identify GFP+ larvae under a fluorescence microscope. Flies lacking *CyO* and *sb* were selected in order to guarantee the $+;\frac{Act5C-GAL4}{+};\frac{UAS-tipE-RNAi}{+}$, $+;+;\frac{nSyb-GAL4}{UAS-tipE-RNAi}$ and $+;\frac{OK6-GAL4}{+};\frac{UAS-tipE-RNAi}{+}$ genotypes were used.

- **RNAi using dicer2**: *tipE* was additionally knocked down, with the use of dicer2, using the $+;\frac{UAS-dicer2}{CyO-GFP};\frac{nSyb-GAL4}{TM6b}$ pan-neuronal driver and the muscle myosin heavy chain driver $+;\frac{UAS-dicer2}{CyO-GFP};\frac{MHC-GAL4}{TM6b}$ crossed to $+;+;\frac{UAS-tipE-RNAi}{TM3,sb}$ to create $+;\frac{UAS-dicer2}{+};\frac{UAS-tipE-RNAi}{nSyb-GAL4}$ and $+;\frac{UAS-dicer2}{+};\frac{UAS-tipE-RNAi}{MHC-GAL4}$ respectively. The *TM6b* balancer chromosome in the $+;\frac{UAS-dicer2}{CyO-GFP}$; $\frac{nSyb-GAL4}{TM6b}$ and $+;\frac{UAS-dicer2}{CyO-GFP};\frac{MHC-GAL4}{TM6b}$ stocks carries the *humeral* (*hu*) gene as a marker, resulting in an increased number of humeral bristles in *Drosophila* adults. In order to ensure $+;\frac{UAS-dicer2}{+};\frac{UAS-tipE-RNAi}{nSyb-GAL4}$ and $+;\frac{UAS-dicer2}{+};\frac{UAS-tipE-RNAi}{MHC-GAL4}$ were correctly used, flies lacking *CyO-GFP*, *TM6b* and *TM3*,*sb* were selected.

V. **Mammalian β1 expression:** $+;\frac{UAS-\beta1EGFP}{CyO-GFP};+$ was crossed to $+;\frac{OK6-GAL4}{CyO-GFP};+$ in order to create $+;\frac{UAS-\beta1EGFP}{OK6-GAL4};+$. GFP+ larvae were selected using a fluorescence microscope in order to ensure $+;\frac{UAS-\beta1EGFP}{OK6-GAL4};+$ were used for both larval locomotor assays and immunohistochemistry in preparation for confocal microscope. GFP+ larvae were only selected if the expression pattern was within the motor

neurons. This was to ensure the GFP signal was not coming from *CyO-GFP*, which is expressed in the gut under the control of the Krüppel promoter.

VI. **Electroretinograms:** *tipE*^{1}*,se* mutants were used during ERGs, with *w+;+;se*^{1} used as a sepia eyed control.

2.6. Temperature shift paralysis assays

Three equidistant horizontal dividing lines were drawn onto the sides of the plastic vials (90 mm height) containing flies. The temperature was increased from room temperature (RT) to 37 °C and the vials photographed once every 60 seconds for 15 minutes using a digital camera. The number of flies located within each quadrant was counted at each timepoint.

2.7. Larval locomotor assays

Locomotor activity of 3rd instar wandering larvae was recorded from above using VirtualDub software and a digital webcam (Creative labs, UK). Two to three larvae of the appropriate genotype were taken from vials. Larvae were taken from vials, washed clean of food using dH_2O and placed onto the centre of a 90 mm diameter petri-dish containing a thin layer (approximately 3 mm depth) of 1% non-nutritive agar and left to acclimatise. Upon initiation of crawling larvae were recorded for 120 s (1 frame s^{-1}). The following locomotor properties were analysed using Fiji (ImageJ):

I. **Mean locomotor velocity:** Videos were batch thresholded and a custom macro was used to track, via the MTrack2 plugin, and plot the larval positions. These data were then used to determine mean locomotor velocity of the larvae.

II. **Tracks and turns:** Fiji was used to create images of larval tracks. Video files were loaded and used to create a Z projection which stacks all video frames into one image. The number of turns made by each larva was calculated manually.

2.8. Vertical climbing assays

Vertical climbing ability of adult flies was assessed using graduated plastic cylinders. Flies were collected at the bottom of the vials by tapping the vial and the percentage of flies at 0-20 mm, 21-40 mm, 41-60 mm and 61-80 mm was calculated 3 seconds after the third "tap". Mean locomotor velocity was calculated manually using the time taken to travel 20 mm. Time was measured using the number of frames taken to travel 20 mm divided by the frame rate of the video.

2.9. Electroretinograms

The ERG method used here is based on that published previously (Hindle *et al.*, 2013). Unanaesthetised seven-day-old flies were aspirated into shortened pipette tips and restrained using nail varnish. Recordings were made between blunt glass pipette electrodes, which contained simple *Drosophila* saline solution (130 mM NaCl, 4.7 mM KCl, 1.9 mM $CaCl_2$). The recording electrode was placed on the centre of the eye, with a reference electrode in the mouthparts. Five stimuli (4 s apart, 750 ms long) were presented, after 2 minutes' adaptation to dark laboratory, from the blue component of LEDs (Onecall; Cat no. 1855508) placed ~ 3 cm in front of the fly. Heating was achieved using an infrared (IR) beam and the temperature at each IR intensity was recorded using a thermocouple. Signals were amplified using a high

impedance (LF356) operational amplifier. Data was collected on an ESP8266 microchip, using the code at https://github.com/wadelab/flyCode/blob/master/collectData/fly_arduino/WebServer/WebServer.ino and analysed in Microsoft Excel.

2.10. Larval dissection and confocal microscopy

Third instar wandering larvae were dissected in PBS, fixed in 3.7% formaldehyde/PBS for 7 min, and washed in PBS (West *et al.*, 2015*b*). Samples were then suspended in 70% glycerol in PBS for 1 hour. Larval preparations were then mounted in Vectashield mounting media. Confocal images were acquired (pinhole: 44μm) using a Zeiss LSM 880 confocal laser scanning microscope with a 40x oil objective lens. Images were post-processed using Fiji (ImageJ).

2.11. Statistical Analysis

4Peaks, nucleotide BLAST and ExPASy were used to analyse sequencing results. GraphPad Prism 7 and Microsoft Excel were used to generate graphs and run statistical tests. Chi squared was used to test for significance between categorical variables. A one-way ANOVA with a post hoc Tukey's was used to test for significance between the means of three or more independent groups. An unpaired *t*-test was used to test for significance between the means of two unmatched groups. Data are presented as mean and SEM. All experiments were repeated independently at least three times. $P < 0.05$ was considered significant.

3. Results

3.1. Behaviour and coordination of *tipE*^{1}*,se* mutants is drastically affected at 37 °C

tipE^{1}*,se* mutant flies have been shown to display a reversible, temperature-sensitive paralytic phenotype at 38 ˚C (Kulkarni & Padhye, 1982). We therefore first sought to confirm that our own *tipE*^{1},*se* stock recapitulated this phenotype in our hands. WT and *tipE*^{1},*se* mutant flies were both subjected to a temperature shift from room temperature to 37 °C (Figure 3.1A, B). WT flies appeared completely unaffected by the shift in temperature, whereas *tipE*^{1},*se* mutant flies exhibited impaired coordination resulting in significantly reduced climbing ability. Although the difference in coordination between the two genotypes was largely apparent, the *tipE*^{1},*se* mutants were not completely paralysed at 37 ˚C, in contrast to previous reports (Feng *et al.*, 1995*a*). Chi squared analysis indicated that loss of coordination in the mutant at 37 °C was highly significant (X^2 (df=2, N=40) = 21.96, $p < 0.001$). However, there was no significant difference between genotypes at RT (X^2 (df=2, N=20) = 3.35, p = 0.1). These results support the notion that the *tipE*^{1}*,se* mutant phenotype is temperature-sensitive. The *tipE* gene from both WT and *tipE*^{1},*se* mutant flies was next amplified and sequenced. The sequencing data confirmed the previously documented T to A transversion point mutation at nucleotide position 714 in *tipE*^{1},*se* mutant flies, resulting in a cysteine residue being changed to a premature STOP codon (Figure 3.1C, D). In summary, these data confirm that our *tipE*^{1}*,se* mutant flies display a temperature-sensitive co-ordination impairment as a result of insertion of a premature STOP

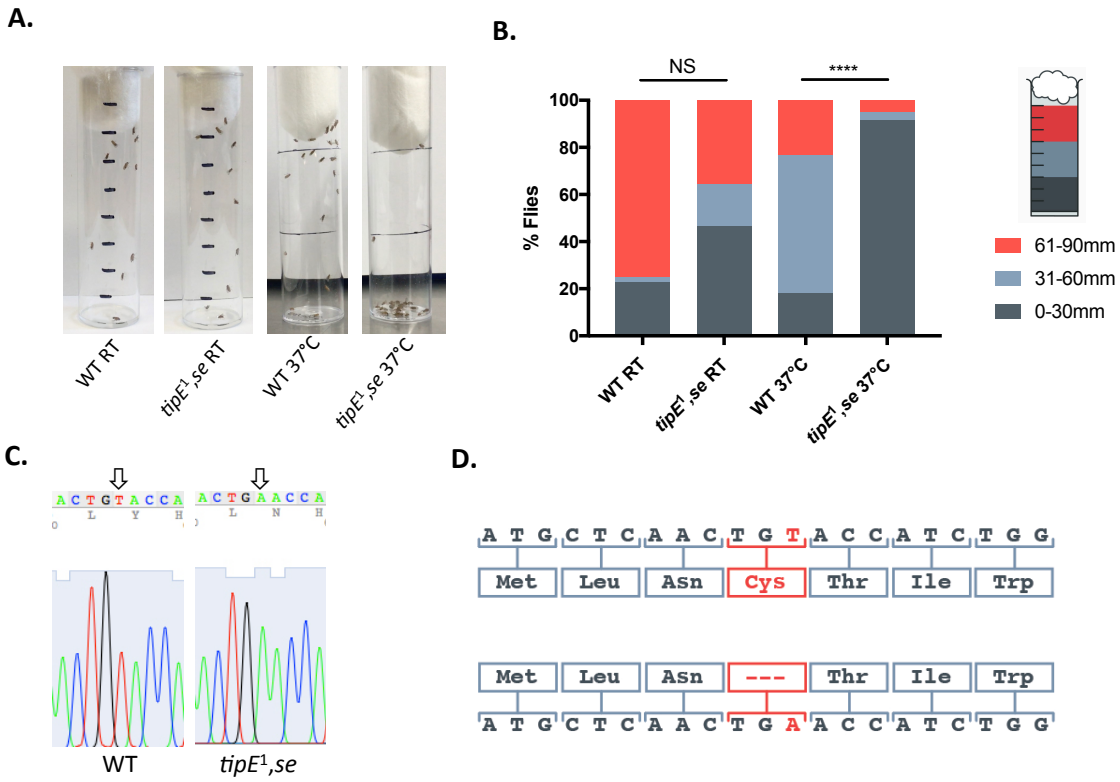

Figure 3.1 – Behaviour and coordination of *tipE*^{1}*,se* mutants is drastically affected at 37 °C.

A. Photographs of flies in marked plastic vials highlighting the effect of temperature shift from RT to 37 °C on behaviour and coordination of WT and *tipE*^{1}*,se* flies. **B.** Percentage of fly population in each region of the vial for WT and *tipE*^{1}*,se* flies at each temperature. Chi squared analysis indicated that loss of coordination between genotypes at 37°C was highly significant (X^2 (df=2, N=40) = 21.96, p < 0.001) and was not significant between genotypes at RT (X^2 (df=2, N=20) = 3.35, p > 0.1). **C.** Chromatogram segment showing a T to A transversion point mutation at nucleotide position 714 in *tipE*^{1}*,se* mutants compared to WT. **D.** Nucleotide and amino acid sequence alignments show the T to A transversion point mutation results in the change of a cysteine residue into a premature STOP codon.

codon; however, the phenotype is not as severe as that reported previously (Feng *et al.*, 1995*a*).

3.2. *tipE*^{1}*,se* mutants indicate a temperature sensitive, reversible decline in visual function

ERGs allow for the measurement of visual function (Hindle *et al.*, 2013). Temperature sensitive paralysis mutants have previously been reported to have reduced on and off ERG transients correlating to an increase in temperature (Kelly & Suzuki, 1974). We therefore sought to test whether the *tipE*^{1}*,se* mutation also results in an ERG phenotype in our flies. The responses to five 750 ms pulses of blue light, 4 seconds apart, were recorded both at ambient temperature (18 °C) and at various raised temperatures (Figure 3.2A). ERG amplitude was measured between the WT fly (*w*$^{+}$*;+;se*^{1}) and *tipE*^{1}*,se* mutants, which both have a sepia coloured eye. Both flies produced consistent ERG traces with no significant difference in ERG peak to peak amplitude (P = 0.27; n = 14; Figure 3.2B). We then measured ERG amplitude in the WT fly at both ambient temperature and at 22 °C. Again, both conditions produced consistent ERG traces with no significant difference in ERG peak to peak amplitude (P = 0.8; n = 7 and 4 respectively; Figure 3.2C). WT flies were not tested at 26 °C due to time constraints.

tipE^{1}*,se* mutants were then subjected to higher temperature increases and several temperature changes in order to determine if higher temperature elicited any effects that were reversible. ERGs were carried out at ambient temperature, then at 22 °C, then returning to ambient temperature, then at 26 °C and finally back at ambient temperature (Figure 3.2D). Elevation to 26 ˚C

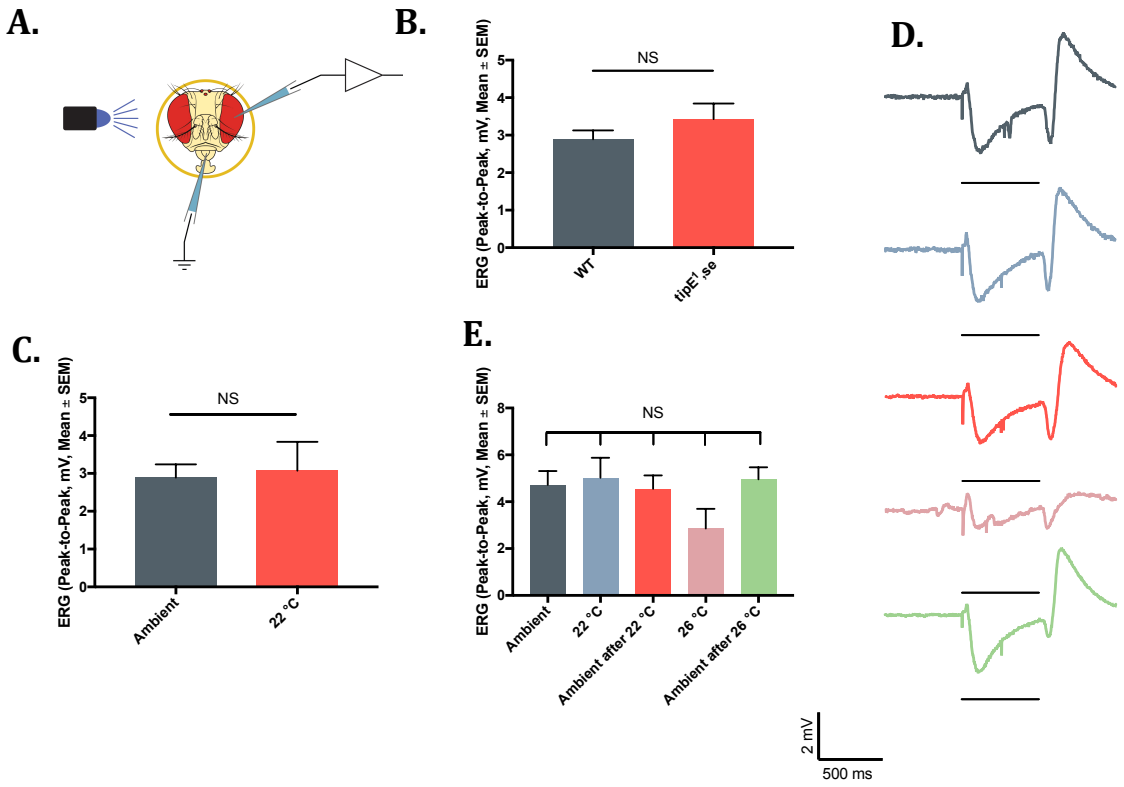

Figure 3.2– *tipE[1],se* mutants display a mild temperature sensitive, reversible decline in visual function

A. Schematic representation of the ERG recording method. An electrical recording is made from the surface of the eye, with a reference electrode in the mouthparts. The responses to five 750 ms pulses of blue light, 4 seconds apart, were recorded. **B.** ERG on-off transient amplitude of WT and *tipE[1],se* mutant flies at ambient temperature (18 ˚C). Unpaired *t* test was used to test for significance (n = 14). **C.** ERG on-off transient amplitude of WT flies at ambient temperature and at 22 °C. Unpaired *t* test was used to test for significance (n = 7 and 4 respectively). WT flies were not tested at 26 °C. **D.** Repeated ERGs from *tipE[1],se* flies at ambient temperature (dark blue), then 22 °C (light blue), then returned to ambient temperature (red), then 26 °C (pink) then returned to ambient temperature (green). The black bar beneath each trace represents the time the light stimulus was on. **E.** ERG on-off transient amplitude of *tipE[1],se* mutant flies at ambient and elevated temperatures. Paired *t* test was used to test for significance (n = 5, other than 22 °C which was n = 4).

notably reduced the peak to peak amplitude of *tipE*^{1}*,se* mutants, however, this was not statistically significant (P = 0.13; n = 5; Figure 3.2E). This reduction was reversed when the files were returned to ambient temperature (Figure 3.2E). In summary, these data suggest that the *tipE*^{1}*,se* mutation mildly reduces visual function at elevated temperatures.

3.3. $+;+;\frac{tipE^{1},se}{Df(3L)GN50}$ exhibit a temperature sensitive phenotype

The *sepia* eye colour mutation is in close proximity to *tipE* on chromosome III and *tipE1,se* mutants carry the *sepia* eye colour mutation (Feng *et al.*, 1995*b*). Sepiapterins are the product of an enzyme known as sepiapterin reductase, which is encoded by the *SPR* gene and is part of the aldo-keto reductase group of enzymes (Ichinose *et al.*, 1991; Persson *et al.*, 2009). Sepiapterin reductase catalyses the NADPH-dependent reduction of various carbonyl substances. Significantly, it catalyses the final steps in the biosynthesis of tetrahydrobopterin (BH_4), an essential cofactor of aromatic amino acid hydroxylases and nitric acid synthases and is thus a rate limiting step in the biosynthesis of various neurotransmitters, such as serotonin, melatonin, dopamine, adrenaline and noradrenaline (Yim *et al.*, 2015).

Drosophila carrying the *sepia* eye colour mutation possess a brown coloured eye as opposed to the wild type red eye produced by pigments called drosopterins (Wiederrecht *et al.*, 1984). Drosopterins are produced by condensation of pyrimidodiazepine (PDA), however, *sepia* mutants produce very little due to being defective in PDA synthase, hence the change of eye colour (Kim *et al.*, 2006). The *sepia* gene encodes PDA synthase and maps

very closely to position 66D on chromosome 3L. In *sepia* mutants, a frameshift mutation in the open reading frame results in a premature STOP codon at nucleotide position 273 of exon 2 (Wiederrecht *et al.*, 1984; Yim *et al.*, 2015). It was therefore necessary to ensure that *sepia* was not the cause, or contributing to, the temperature sensitive paralysis seen in *tipE[1],se* mutants.

The *Drosophila* community has created a valuable "complete deficiency kit" that covers the majority of the *Drosophila* genome. First described in 1917, the term deficiency refers to the deletion of a continuous chromosomal region, containing numerous genes, that is "definite and measurable" (Bridges, 1917). By using a specific deletion to uncover a gene of interest, a definitive null allele is created, which can then be analysed further. Typically, such deficiency lines are used in order to gauge the severity of a phenotype in homozygous flies of novel mutation compared to hemizygous flies carrying the deficiency (the mutant allele in trans to the deficiency). In addition to this, deficiencies allow for mutation mapping to a near specific region of the genome by carrying out a simple complementation test (Ryder *et al.*, 2007; Roote & Russell, 2012). *tipE[1],se* mutant flies were crossed to the deficiency line $+;+;\frac{Df(3L)GN50}{TM8}$ to create $+;+;\frac{tipE^{1},se}{Df(3L)GN50}$ in order to investigate whether *sepia* was causing or contributing to the temperature sensitive phenotype. A paralysis assay carried out at 37 °C showed that $+;+;\frac{tipE^{1},se}{Df(3L)GN50}$ flies exhibit a temperature sensitive coordination impairment phenotype comparable to that of *tipE[1],se* mutants (Figure 3.3A, B). Again, the *tipE[1],se* and the $+;+;\frac{tipE^{1},se}{Df(3L)GN50}$ flies were not completely paralysed, although they were highly uncoordinated. WT and $+;+;\frac{Df(3L)GN50}{TM8}$ flies were

unaffected by the temperature shift, suggesting that it is a mutation at the *tipE* locus, rather than the *sepia* locus, which is responsible for the temperature-sensitive coordination impairment phenotype (Figure 3.3A, B). In addition, $\frac{w^-}{+}; +; \frac{tipE^1,se}{+}$ were also phenotypically normal, suggesting that a heterozygous *tipE[1],se* mutation is not sufficient to induce coordination impairment (Figure 3.3A, B). In summary, these data suggest that it is the *tipE* mutation rather than the *sepia* mutation which is responsible for coordination impairment. This result is novel and supports the argument that *tipE* is responsible for regulating VGSC-mediated neuronal activity and thus neurological function.

3.4. *tipE[1],se* mutant larvae and adults and $+; +; \frac{tipE^1,se}{Df(3L)GN50}$ adults exhibit additional physiological deficits

Given the robust motor coordination phenotype that we observed for the adult *tipE[1],se* mutant flies, we reasoned that motor impairment may also be evident earlier on in development. Therefore, to provide an additional functional, behavioral readout of NMJ activity at an earlier developmental stage, larval locomotor assays were carried out. Mean locomotor velocity of WT and *tipE*[1],*se* mutant third instar wandering larvae was recorded for 120 seconds at RT (Figure 3.4A, B). *tipE*[1],*se* mutant larvae had a significantly reduced mean locomotor velocity of 0.56 ± 0.03 mm/s compared to WT mean locomotor velocity of 0.69 ± 0.02 mm/s ($P < 0.05$). This result is novel and suggests that the *tipE[1],se* mutation may cause minor motor impairment at non permissive temperatures. The locomotor velocity was notably much further reduced in the *tipE*[1],*se* mutant larvae at 37 °C (0.25 ± 0.06 mm/s) compared to WT larvae at

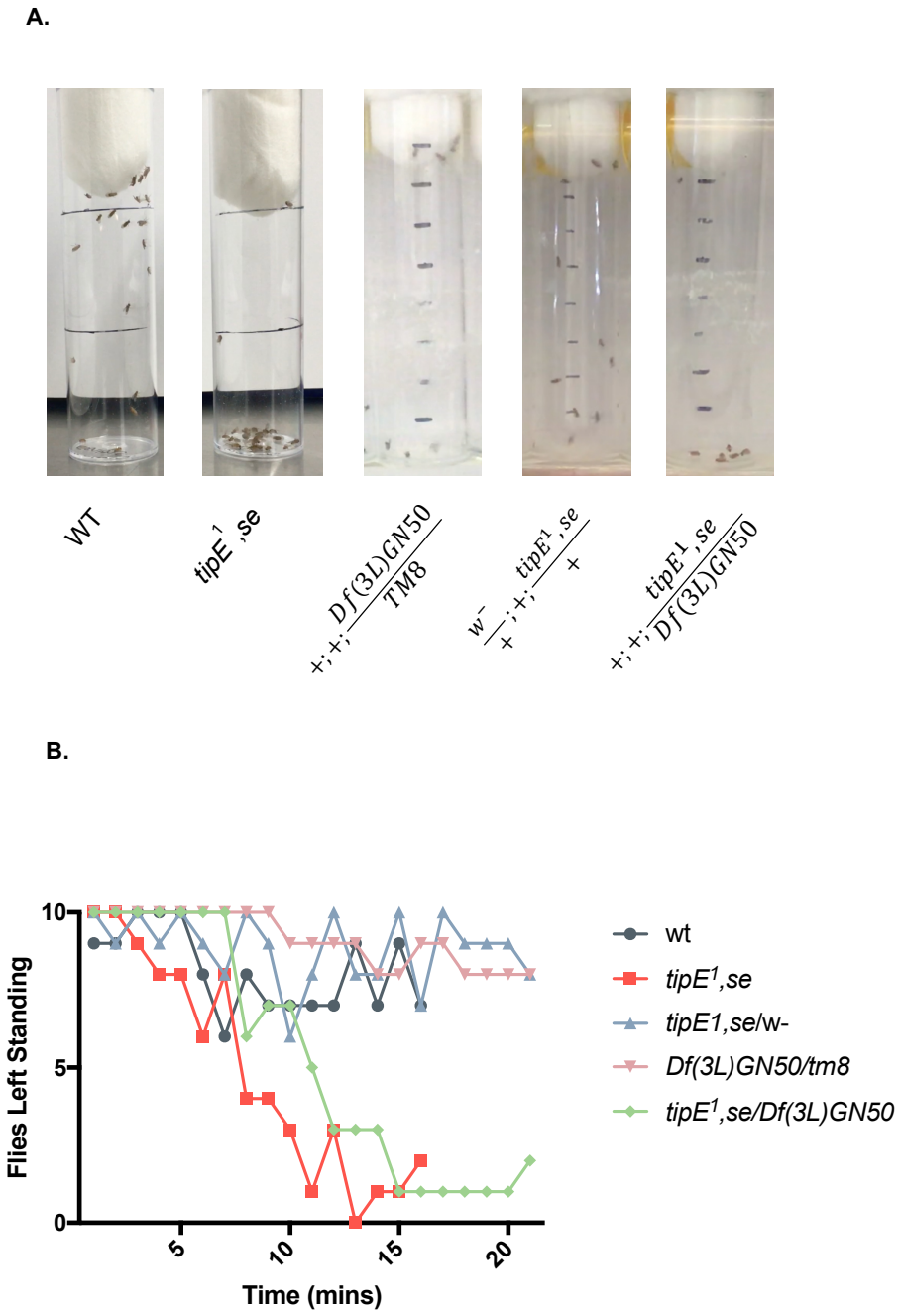

Figure 3.3 – +; +; $\frac{tipE^1,se}{Df(3L)GN50}$ exhibit a temperature sensitive phenotype.

A. Photographs of WT, *tipE*^{1},*se*, $\frac{w^-}{+}$; +; $\frac{tipE^1,se}{+}$, +; +; $\frac{Df(3L)GN50}{TM8}$ and +; +; $\frac{tipE^1,se}{Df(3L)GN50}$ flies at 37 °C. **B.** The number of flies left standing after the indicated timepoints in a paralysis assay at 37 °C. The data show that *tipE*^{1},*se* mutants and +; +; $\frac{tipE^1,se}{Df(3L)GN50}$ flies have an uncoordinated phenotype. WT, +; +; $\frac{Df(3L)GN50}{TM8}$ and $\frac{w^-}{+}$; +; $\frac{tipE^1,se}{+}$ are unaffected by an increase in temperature to 37 °C (N=10/group).

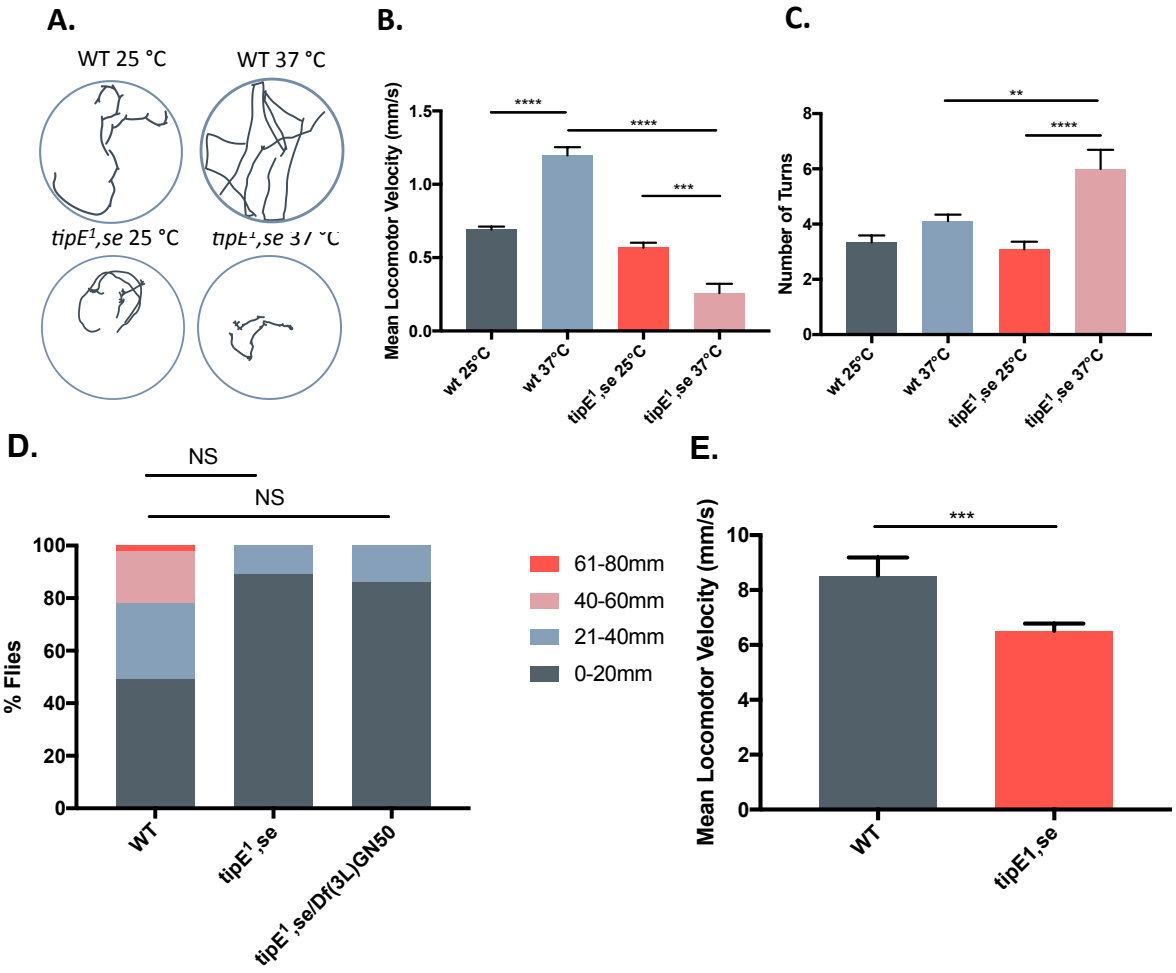

Figure 3.4 – *tipE*^{1}, *se* mutant larvae and adults exhibit physiological deficits. **A.** Traces of larval crawling tracks for WT and *tipE*^{1},*se* third instar wandering larvae at 25 and 37 ˚C. **B.** Mean locomotor velocity of WT and *tipE*^{1},*se* third instar wandering larvae. A one-way ANOVA with a post hoc Tukey's was used to test for significance. n=37, 37, 38, 13 respectively. **C.** Mean number of turns made by WT and *tipE*^{1}, *se* mutant larvae. A one-way ANOVA with a post hoc Tukey's was used to test for significance. n=48, 54, 37, 14 respectively. **D.** Adult fly climbing assay showing percentage of flies climbing to each indicated position in the vial for WT, *tipE*^{1}, *se* and +; +; $\frac{tipE^1,se}{Df(3L)GN50}$ at RT. Chi squared analysis was used to test for significance: WT vs. *tipE*^{1}, *se* (X^2(df=3, n=20) = 4.21, p > 0.2) WT vs. +; +; $\frac{tipE^1,se}{Df(3L)GN50}$ (X^2(df=3, n=20) = 3.73, p > 0.3). **E.** Mean locomotor velocity (mm/s) for WT and *tipE*^{1},*se* mutant flies. Mean locomotor velocity was calculated manually using the time taken to travel 20 mm. Time was calculated using the number of frames taken to travel 20 mm divided by the frame rate of the video. Unpaired *t* test was used to test for significance, * p<0.05; *** p≤ 0.001; **** p≤ 0.0001; NS, not significant.

37 °C (1.20 ± 0.05 mm/s; P <0.0001), highlighting the early developmental onset of the more severe temperature sensitive motor impairment.

It has been shown that the number of turns made by crawling larvae, defined as a pause followed by a directional change of the head, is increased when the animals are stressed and negatively correlates to mean locomotor velocity (Günther *et al.*, 2016). We therefore next calculated the number of turns manually using Fiji (ImageJ). The number of turns made by *tipE*^{1},*se* mutant larvae almost doubled at 37 °C (6.0 ± 0.68) compared to 25 °C (3.08 ± 0.28; P < 0.001; Figure 3.4C) and was significantly higher than WT at 37 °C (4.11 ± 0.23; P < 0.01). There was no difference between WT (3.33 ± 0.25) and *tipE*^{1}*,se* at 25 °C (P = 0.81; Figure 3.4C). Thus, the *tipE*^{1},*se* mutation increases the number of turns at elevated temperature, but not at RT. Together, these results suggest that number of turns may be a less sensitive measure of locomotor deficit than velocity.

Drosophila adult flies possess an innate survival response in which they perform negative geotaxis as a result of being tapped to the bottom of a collection vial. This geotaxic response can be analysed to determine potential physiological deficits in mutant genotypes, for example *tipE*^{1},*se* mutants (Gargano *et al.*, 2005). Vertical climbing ability of adult WT*, tipE*^{1},*se* and $+;+;\frac{tipE^{1},se}{Df(3L)GN50}$ flies was calculated by performing a negative geotaxis climbing assay at RT (Figure 3.4D). Flies were given a single opportunity to perform negative geotaxis in graduated plastic cylinders, following three sharp taps of the cylinder in order to collect them at the bottom. The position of each fly within

the cylinder was recorded 3 seconds after the final tap. The climbing ability of *tipE*^{1},*se* mutants and $+;+;\frac{tipE^{1},se}{Df(3L)GN50}$ appeared to be marginally negatively affected compared to that of the WT control however this was not significant (WT vs. *tipE*^{1},*se* χ^2 (df=3, n=20) = 4.21, p > 0.2; WT vs. $+;+;\frac{tipE^{1},se}{Df(3L)GN50}$ χ^2 (df=3, n=20) = 3.73, p > 0.3; Figure 3.4D). Finally, we measured the mean locomotor velocity of adult flies over a distance of 20 mm recorded in the climbing assay at RT. The mean locomotor velocity of WT flies was 8.5 ± 0.66 mm/s. The mean locomotor velocity of *tipE*^{1}*,se* flies was significantly reduced (6.5 ± 0.26 mm/s; P < 0.001; n = 41 and 86 respectively; Figure 3.4E).

In summary, these data show that *tipE* is critical for normal motor function. In addition, the *tipE*^{1}*,se* mutation results in a mild locomotor deficit at normal temperature in both larvae and adult flies. However, the deficit is more severe at elevated temperature.

3.5. *tipE* knockdown by RNAi increases climbing ability at room temperature

The preceding data suggest that the *tipE*^{1}*,se* mutation may function either as a null mutant or as a dominant negative at elevated temperature. In order to separate these possibilities, we next sought to downregulate wildtype *tipE* using RNAi. We reasoned that if the *tipE*^{1}*,se* mutation functions as a null mutant, RNAi knockdown of wildtype *tipE* could generate a similar phenotype. To do this, we took advantage of an RNAi line generated by the transgenic RNAi project (TRiP) established by Harvard Medical School (Perkins *et al.*, 2015). To date, TRiP has generated numerous transgenic flies containing an RNAi hairpin

that has been placed under the control of UAS-GAL4. Transgenes that contain the hairpin loop are inserted via site specific recombination, a technique harnessing the powers of recombinase enzymes to manipulate gene structure and control gene expression (Groth *et al.*, 2004). As part of the TRiP project, a series of vectors were created under the name Valium (*Vermilion-AttB-Loxp-intron-UAS-MCS*) in order to integrate the RNA hairpin into the flies. Valium10 is a modified version of Valium vector that has been optimised in order to provide a more effective knockdown. This has been achieved by the inclusion of insulator sequences, known as *gypsy* insulators, which significantly increase hairpin expression (Ni *et al.*, 2009).

The TRiP RNAi line $+;+;\frac{UAS-tipE-RNAi}{TM3,sb}$ was crossed (without dicer2) to a global driver $(+;\frac{Act5C-GAL4}{CyO-GFP};+)$, a pan-neuronal driver $(+;+;\frac{nSyb-GAL4}{CyO-GFP})$ and a motor-neuronal driver $(+;\frac{OK6-GAL4}{CyO-GFP};+)$ in order to knock down *tipE* expression in the respective tissues, creating the genotypes $+;\frac{Act5C-GAL4}{+};\frac{UAS-tipE-RNAi}{+}$, $+;+;\frac{nSyb-GAL4}{UAS-tipE-RNAi}$ and $+;\frac{OK6-GAL4}{+};\frac{UAS-tipE-RNAi}{+}$. A negative geotaxis climbing assay was carried out on these stocks at room temperature. Surprisingly, there was a general trend towards a slightly increased climbing ability in the three *tipE*-RNAi lines compared to WT control flies. However, χ^2 analysis indicated that this was not statistically significant (χ^2 (df=6, N=50) = 8.4, p = 0.20; Figure 3.5A). The effectiveness of RNAi-mediated target knockdown can be improved by overexpressing the RNase III double-stranded RNA-specific endonuclease

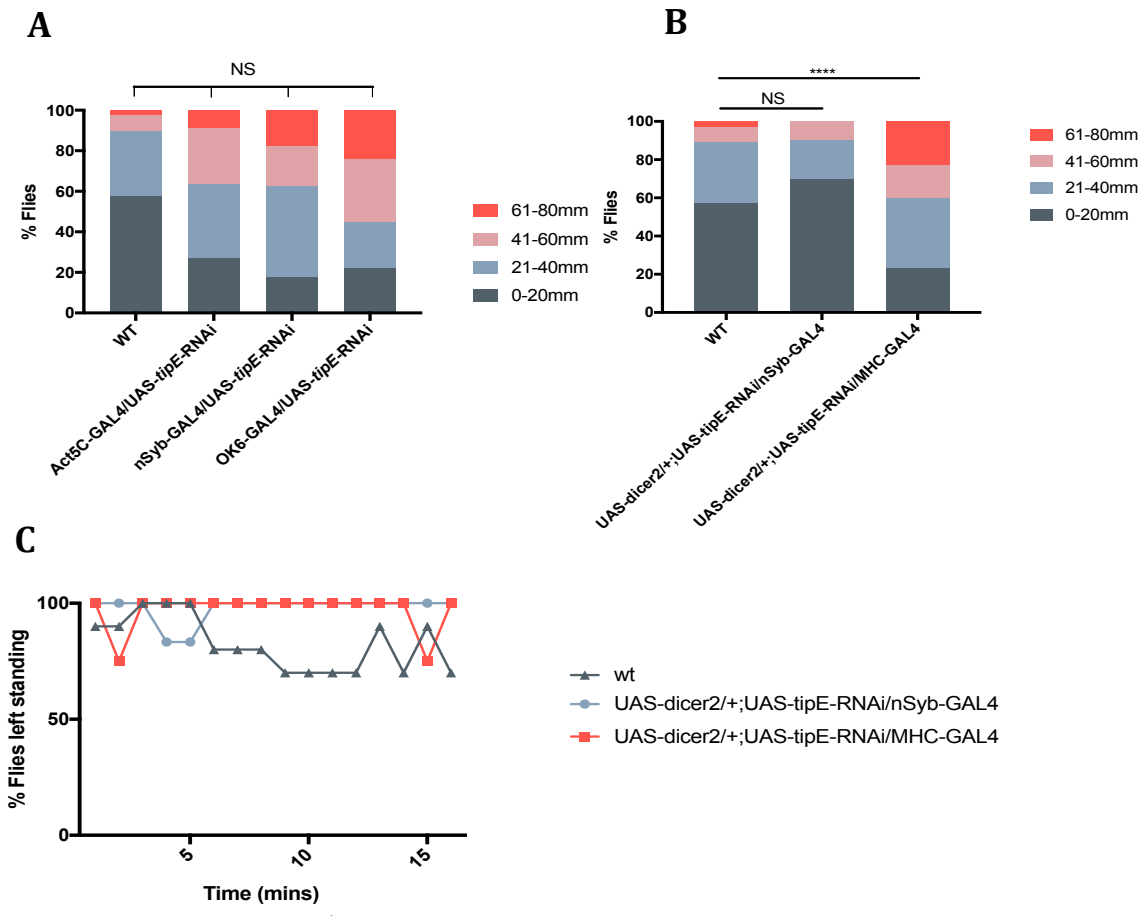

Figure 3.5 – *tipE* knockdown by RNAi increases climbing ability at room temperature.

A. Results of climbing assay at RT showing % of flies reaching each indicated region of the vial for stocks in which *tipE* was knocked down by RNAi (without dicer2) globally ($+;\frac{Act5C-GAL4}{+};\frac{UAS-tipE-RNAi}{+}$), pan-neuronally ($+;+;\frac{nSyb-GAL4}{UAS-tipE-RNAi}$) and in the motor neurons ($+;\frac{OK6-GAL4}{+};\frac{UAS-tipE-RNAi}{+}$). Chi squared analysis indicated that climbing ability between genotypes was not significant (χ^2 (df=6, N=59) = 8.4, p = > 0.20). **B.** Results of climbing assay at RT showing % of flies reaching each indicated region of the vial for stocks in which *tipE* was knocked down in the presence of dicer2, driven pan-neuronally ($+;\frac{UAS-dicer2}{+};\frac{UAS-tipE-RNAi}{nSyb-GAL4}$) and using the muscle myosin heavy chain (MHC) driver ($+;\frac{\mathrm{UAS-dicer2}}{+};\frac{\mathrm{UAS-}tipE\mathrm{-RNAi}}{\mathrm{MHC-GAL4}}$). *tipE* RNAi using dicer2 driven by MHC-GAL4 increased climbing ability at room temperature (χ^2 (df=3, N=16) = 33.44, p < 0.0001). However, *tipE* RNAi using dicer2 driven pan-neuronally had no effect compared to WT (χ^2 (df=3, N=14) = 7.322, p > 0.05). **C.** Results of paralysis assay at 37 °C for $+;\frac{UAS-dicer2}{+};\frac{UAS-tipE-RNAi}{nSyb-GAL4}$ and $+;\frac{UAS-dicer2}{+};\frac{UAS-tipE-RNAi}{MHC-GAL4}$ flies showing lack of effect of elevated temperature.

dicer2 (Kim *et al.*, 2005). Therefore, next, *tipE* was additionally knocked down in the presence of dicer2, using the $+;+;\frac{nSyb-GAL4}{CyO-GFP}$ pan-neuronal driver and the muscle myosin heavy chain driver $+;+;\frac{MHC-GAL4}{CyO-GFP}$ to create $+;\frac{UAS-dicer2}{+}$; $\frac{UAS-tipE-RNAi}{nSyb-GAL4}$ and $+;\frac{UAS-dicer2}{+}$; $\frac{UAS-tipE-RNAi}{MHC-GAL4}$. We used $+;\frac{UAS-dicer2}{+};\frac{UAS-tipE-RNAi}{MHC-GAL4}$ as a control for off target effects of the RNAi. A climbing assay using these flies at room temperature revealed that muscle-specific *tipE* knockdown in the presence of dicer2 significantly increased climbing ability (χ^2 (df=3, N=16) = 33.44, $p < 0.0001$; Figure 3.5B). However, there was no significant difference in the climbing ability of flies when *tipE* RNAi and dicer2 were driven pan-neuronally, compared to WT ($P > 0.05$; Figure 3.5B). These results suggest that the addition of dicer2 increases RNAi-mediated knockdown of *tipE.* In addition, the data suggest that whilst the neuronally-expressed *tipE* protein plays a minimal functional role in regulating climbing behaviour at room temperature, *tipE* expression in muscle appears to negatively regulate climbing behaviour.

We next investigated the effect of knocking down *tipE* on temperature-dependent paralysis. A paralysis assay at 37 °C revealed that $+;\frac{UAS-dicer2}{+};\frac{UAS-tipE-RNAi}{nSyb-GAL4}$ and $+;\frac{UAS-dicer2}{+};\frac{UAS-tipE-RNAi}{MHC-GAL4}$ were unaffected by the increase in temperature (Figure 3.5C). This result suggests that although *tipE* knockdown in muscle affects climbing behaviour, it has no effect on temperature-sensitive motor behaviour or paralysis. This result is in direct contrast to the data from the *tipE^1,se* mutant and provides novel evidence to suggest that the *tipE^1,se* mutation may function as a dominant negative rather

than a functional null, though this is contradicted by the lack of paralysis in a *tipE*^{1}*,se* heterozygote (Figure 3.3B). The efficiency of mRNA downregulation by RNAi or RNAi in the presence of dicer 2 was not determined.

3.6. Mammalian β1 expresses ectopically in neuronal cell bodies in the *Drosophila* larval brain

β1 is widely expressed in the mammalian CNS, both at the plasma membrane and intracellularly, in both neurons and astroglia (Aronica *et al.*, 2003; Chen *et al.*, 2004; Brackenbury *et al.*, 2010; Nguyen *et al.*, 2012). In order to evaluate β1 localisation when expressed in *Drosophila* motor neurons under control of $+;\frac{OK6-GAL4}{CyO-GFP};+$, we next studied β1-EGFP fluorescence in third instar wandering larvae using confocal microscopy. Larvae of the genotype $+;\frac{UAS-\beta1EGFP}{OK6-GAL4};+$ were dissected in PBS, fixed in 3.7% formaldehyde/PBS and visualised using a confocal microscope. Mammalian β1, driven by the $+;\frac{OK6-GAL4}{CyO-GFP};+$ motor neuronal driver, was found to be highly expressed in neuronal cell bodies within the *Drosophila* larval brain (Figure 3.6). This result confirms that the transgene can be ectopically expressed in the nervous system, as expected.

3.7. Mammalian β1 expression has no effect on larval mean locomotor velocity at 25 °C but does increase number of directional turns

Given that *Drosophila tipE* and mammalian β1 both modulate Na^{+} current carried by VGSCs, we reasoned that β1 may recapitulate the effect of *tipE* on motor behaviour. We therefore sought to investigate whether β1 could rescue the *tipE*^{1}*,se* mutant phenotype. As a preliminary experiment prior to attempting

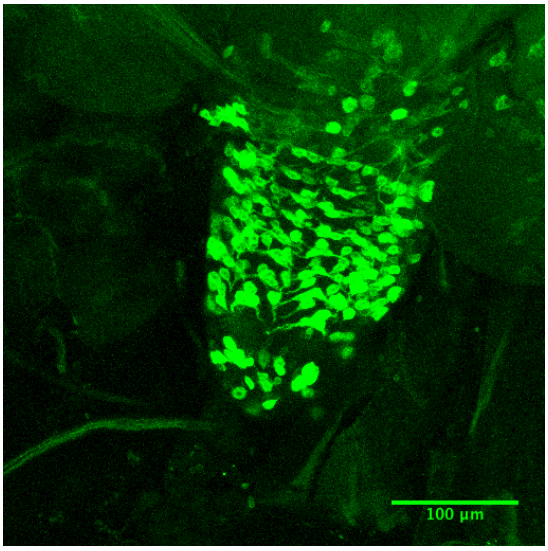

Figure 3.6 - Mammalian β1 expresses ectopically in neuronal cell bodies in the *Drosophila* larval brain.

Dissected mount of *Drosophila* larval brain expressing mammalian β1-EGFP in the motor neurons $(+;\frac{UAS-\beta 1EGFP}{OK6-GAL4};+)$. β1 is expressed in neuronal cell bodies. Image taken on a Zeiss LSM 880 confocal microscope at 40x magnification.

to rescue the *tipE* knock down phenotype with expression of β1, we tested the effect of expressing β1 alone on physiological function in the nervous system of WT files. The rat β1 subunit fused to EGFP at the intracellular C-terminus (Chioni *et al.*, 2009) was cloned into the pUAST vector. This was then microinjected into fly embryos to create a UAS-β1EGFP line. A cross was set up to drive the expression of β1 in motor neurons using $+;\frac{OK6-GAL4}{CyO-GFP};+$. The mean locomotor velocity of$+;\frac{UAS-\beta1EGFP}{OK6-GAL4};+$ third instar wandering larvae was then recorded compared to WT control larvae. Locomotor velocity was unaffected by motor neuronal expression of β1 at 25 °C (0.68 ± 0.04 mm/s for β1 vs. 0.69 ± 0.02 mm/s for WT; n = 37 and 13 respectively; P = 0.99; Figure 3.7A, B). However, $+;\frac{UAS-\beta1EGFP}{OK6-GAL4};+$ third instar wandering larvae had a decreased mean locomotor velocity of 0.51 ± 0.06 mm/s at 37 °C, which was significantly different to both lines at RT and to WT at 37 °C (1.20 ± 0.05 mm/s; P < 0.0001) (Figure 3.7A, B). The number of turns made by $+;\frac{UAS-\beta1EGFP}{OK6-GAL4};+$ third instar wandering larvae more than doubled at 25 °C (6.41 ± 0.56 turns; n = 17; P < 0.0001) and 37 °C (7.57 ± 0.73 turns; n = 14; P < 0.0001) compared to WT larvae at 25 °C (3.33 ± 0.25 turns; n = 48; Figure 3.7C). In summary, these results suggest that β1 expression in *Drosophila* motor neurons moderately inhibits motor co-ordination, evidenced by increased turning behaviour (Günther *et al.*, 2016).

3.8 Rescue of *tipE1,se* mutant phenotype using mammalian β1

Given the functional similarity between *tipE* and mammalian β1 in modulating Na^+ current (Feng *et al.*, 1995*a*; McEwen *et al.*, 2004*a*), the final goal was to

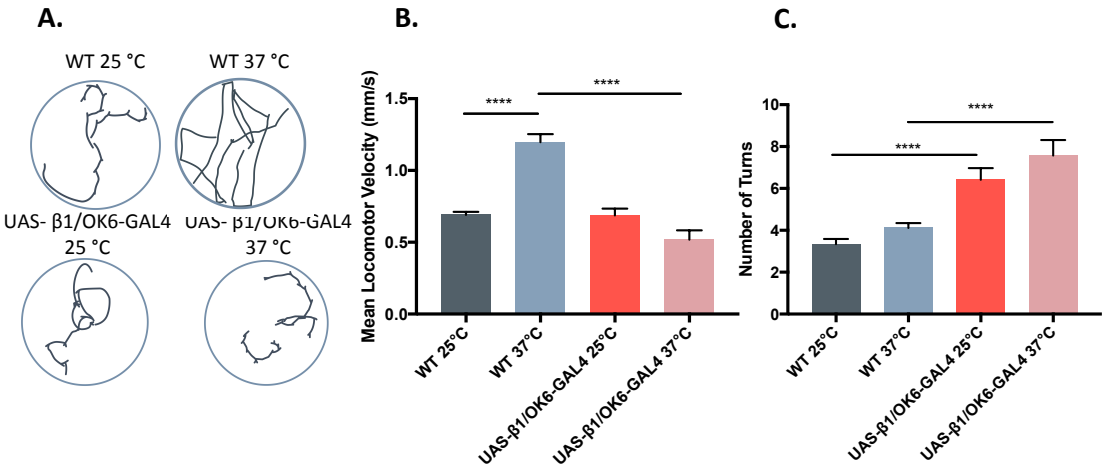

Figure 3.7 - Mammalian β1 expression increases larval turns

A. Traces of larval crawling tracks for WT and $+;\frac{UAS-\beta1EGFP}{OK6-GAL4};+$ third instar wandering larvae at 25 and 37 ˚C. **B.** Mean locomotor velocity of WT and $+;\frac{UAS-\beta1EGFP}{OK6-GAL4};+$ third instar wandering larvae (n = 37, 37, 13, 17 respectively). **C.** Mean number of turns made by WT and $+;\frac{UAS-\beta1EGFP}{OK6-GAL4};+$ larvae (n = 48, 54, 37, 14 respectively). A one-way ANOVA with a post hoc Tukey's was used to test for significance. *P < 0.05; **P < 0.01; ***P < 0.001; ****P< 0.0001; NS, not significant.

attempt to rescue the *tipE[1],se* phenotype by expressing β1. We aimed to utilise advanced *Drosophila* genetics to create the final experimental fly $+;\frac{UAS-\beta1EGFP}{nSyb-GAL4};\frac{tipE^{1},se}{Df(3L)GN50}$. Mammalian β1, under the control of UAS, would be driven pan-neuronally by *nSyb-GAL4* (on the second chromosome), in a $+;+;\frac{tipE^{1},se}{Df(3L)GN50}$ background fly. This would be done by first creating the following flies:

I. $+;\boldsymbol{\frac{UAS-\beta1EGFP}{CyO-GFP}};\boldsymbol{\frac{TM6b}{MKRS}}$ **:** $+;\frac{UAS-\beta1EGFP}{CyO-GFP};+$ would be crossed to the double balancer (DB) $+;\frac{If}{CyO-GFP};\frac{TM6b}{MKRS}$ to first create $+;\frac{UAS-\beta1EGFP}{CyO-GFP};\frac{+}{MKRS}$, which would then be crossed back to the DB to finally create $+;\frac{UAS-\beta1EGFP}{CyO-GFP};\frac{TM6b}{MKRS}$.

II. $+;\boldsymbol{\frac{nSyb-GAL4}{CyO-GFP}};\boldsymbol{\frac{TM6b}{MKRS}}$ **:** $+;\frac{nSyb-GAL4}{CyO-GFP};+$ would be crossed to the DB to first create $+;\frac{nSyb-GAL4}{CyO-GFP};\frac{+}{MKRS}$, which would then be crossed back to the DB to finally create $+;\frac{nSyb-GAL4}{CyO-GFP};\frac{TM6b}{MKRS}$.

III. $+;\boldsymbol{\frac{If}{CyO-GFP}};\boldsymbol{\frac{tipE^{1},se}{TM6b}}$ **:** *tipE[1],se* would be crossed to the DB to first create $+;\frac{+}{CyO-GFP};\frac{tipE^{1},se}{TM6b}$, which would then be crossed back to the DB to finally create $+;\frac{If}{CyO-GFP};\frac{tipE^{1},se}{TM6b}$.

IV. $+;\frac{\boldsymbol{If}}{\boldsymbol{CyO-GFP}};\frac{\boldsymbol{Df(3L)GN50}}{\boldsymbol{TM6b}}$ **:** $+;+;\frac{Df(3L)GN50}{TM8}$ would be crossed to the DB to first create $+;\frac{+}{CyO-GFP};\frac{Df(3L)GN50}{TM6b}$, which would then be crossed back to the DB to finally create $+;\frac{If}{CyO-GFP};\frac{Df(3L)GN50}{TM6b}$.

Once the above flies had been created, they would be crossed in the following way to produce the following flies:

V. $+;\frac{\boldsymbol{nSyb}}{\boldsymbol{CyO-GFP}};\frac{\boldsymbol{Df(3L)GN50}}{\boldsymbol{TM6b}}$ **:** $+;\frac{If}{CyO-GFP};\frac{Df(3L)GN50}{TM6b}$ would be crossed to $+;\frac{nSyb-GAL4}{CyO-GFP};\frac{TM6b}{MKRS}$ to create $+;\frac{nSyb}{CyO-GFP};\frac{Df(3L)GN50}{TM6b}$.

VI. $+;\frac{\boldsymbol{UAS-\beta 1EGFP}}{\boldsymbol{CyO-GFP}};\frac{\boldsymbol{tipE^{1},se}}{\boldsymbol{TM6b}}$: $+;\frac{UAS-\beta 1EGFP}{CyO-GFP};\frac{TM6b}{MKRS}$ would be crossed to $+;\frac{If}{CyO-GFP};\frac{tipE^{1},se}{TM6b}$ to create $+;\frac{UAS-\beta 1EGFP}{CyO-GFP};\frac{tipE^{1},se}{TM6b}$.

VII. $+;\frac{\boldsymbol{UAS-\beta 1EGFP}}{\boldsymbol{nSyb-GAL4}};\frac{\boldsymbol{tipE^{1},se}}{\boldsymbol{Df(3L)GN50}}$ **:** $+;\frac{UAS-\beta 1EGFP}{CyO-GFP};\frac{tipE^{1},se}{TM6b}$ would be crossed to $+;\frac{nSyb}{CyO-GFP};\frac{Df(3L)GN50}{TM6b}$ to create the final experimental fly $+;\frac{UAS-\beta 1EGFP}{nSyb-GAL4};\frac{tipE^{1},se}{Df(3L)GN50}$.

However, unfortunately, it was not possible to complete these crosses before the submission deadline for this thesis. Steps I-IV were completed however, in the case of some genotypes, an inadequate number of females emerged. This meant males from said genotype had to be crossed back to the DB in order to try and produce more females of the required genotype. This subsequently

delayed further crosses. It is planned for another member of the lab to complete this aspect of the project.

4. Discussion

Our data show that the *tipE*^{1}*,se* mutant is reversibly temperature sensitive at 37 °C. In addition to this, we also found a physiological locomotor deficit in both *tipE*^{1}*,se* mutant adults and larvae, which is exacerbated by an increase in temperature. Furthermore, although we found no significant difference in ERG amplitude between *tipE*^{1}*,se* mutants and WT at ambient temperature, we did see an evident trend towards decreased ERG amplitude at elevated temperatures. Surprisingly, a climbing assay at room temperature indicated that *tipE* knockdown by RNAi and dicer2 in the muscle resulted in an increased climbing ability and hyperactivity at room temperature. In contrast, the RNAi-dicer2 expressing flies did not show a temperature sensitive phenotype. Mammalian β1 expression had no effect on larval locomotor velocity, however, did increase the number of turns at 25 °C, suggesting a mild physiological impairment.

4.1. *tipE*^{1}*,se* mutants exhibit a physiological deficit which is exacerbated by an increase in temperature.

To date, no mammalian β subunit orthologues have been discovered in *Drosophila,* however evidence suggests that *Drosophila tipE*, located on chromosome III, is a VGSC auxiliary subunit (Kulkarni & Padhye, 1982; Warmke *et al.*, 1997; Littleton & Ganetzky, 2000; Hodges *et al.*, 2002). Thus, this membrane protein could essentially be a functional orthologue of the mammalian VGSC β1 subunit. *tipE*^{1}*,se* mutants have previously been shown to exhibit a temperature sensitive phenotype, suggesting the importance of *tipE* in regulating neuronal excitability (Wang *et al.*, 2013). In addition to this, it has

been suggested that due to the decrease in VGSC numbers and Na^+ current, the regulation of VGSC function is affected by the *tipE* gene product (Feng *et al.*, 1995*b*). This may be as a result of direct physical interaction of the *tipE* gene product with the VGSC α subunit, mirroring the mechanism of action of mammalian β subunits (Isom *et al.*, 1994).

Previous research into the phenotype of the *tipE^1,se* mutant has shown that it is reversibly temperature sensitive at 38 °C, resulting in a paralysed state (Kulkarni & Padhye, 1982; Feng *et al.*, 1995*a*). The term "paralysis" was defined as the fraction of flies not left in a standing posture after the vial was gently tapped (Siddiqi & Benzer, 1976). It is unclear whether flies reported to be in a paralysed state were completely paralysed, and therefore unable to move at all, or simply severely uncoordinated, causing them to fall in the vial. In the present study, we found that the *tipE^1,se* mutants were severely uncoordinated but not paralysed. This discrepancy may be due to inaccurate reporting of paralysis in the previous study (Kulkarni & Padhye, 1982). Alternatively, it is possible that the *tipE^1,se* mutants were previously exhibiting temperature induced paralysis. However, over the intervening 23 years since that study, this may have attenuated to an uncoordinated phenotype, as a result of accumulation of phenotype-altering genetic modifiers in the stock. The latter possibility is supported by a further discrepancy in the larval phenotype: previous research found *tipE^1,se* mutant 3rd instar wandering larvae to paralyse, defined as a complete absence of body movement, after 30 seconds at a permissive temperature (Kulkarni & Padhye, 1982). Although we found that an increase in temperature from 25 °C to 37 °C decreased locomotor velocity and increased the number of turns, we did not observe any paralysis within *tipE^1,se* mutant 3rd

instar wandering larvae. Further work is required to definitively establish whether additional modifiers have indeed altered the phenotype of the *tipE1,se* stock.

The reversibility of the temperature-induced phenotype in *tipE*^{1}*,se* flies is analogous to the symptoms of myoplegia paroxysmalis familiaris and periodic paralysis (Sugiura *et al.*, 2000). An autosomal dominant myopathy, periodic paralysis describes a group of rare genetic diseases that have been found to have common triggers, which include an increase in temperature (Aoki *et al.*, 2000; Sugiura *et al.*, 2000). Mutations within the VGSC are among the most common causes behind periodic paralysis (Ghovanloo *et al.*, 2018). The underlying mechanism is a malfunction of $Na_v1.4$ in the skeletal muscle cell membrane which ultimately results in hyperactivity and prolongs action potentials and refractory periods, bringing about periodic bouts of myotonia and paralysis (Jurkat-Rott & Lehmann-Horn, 2010).

VGSC gating is temperature sensitive, with activation, inactivation and both fast and slow activation increasing at higher temperatures (Pröbstle *et al.*, 1988; Ruff, 1999; Thomas *et al.*, 2009). This change in rate is unsurprising, as an increase in thermal energy will result in a lower activation energy required to conformationally change proteins and can be described by the temperature coefficient Q_{10}. Once the change in temperature drastically falls below or drastically exceeds that of normothermia, the body is less able to cope with such changes and as a result can cause convulsive effects and myotonia (Egri & Ruben, 2012). Thus, if *tipE* is required for normal VGSC gating, the temperature-sensitive mutation may alter channel properties at elevated

temperatures. Voltage-clamp experiments would be required to investigate this possibility. Results from our larval crawling assays and adult negative geotaxis climbing assays suggested that *tipE*^{1},*se* mutants also exhibit a subtle physiological deficit at room temperature. This is a novel finding which has not been previously reported. However, the mechanistic basis for this phenotype is not clear.

We found that there was no significant difference in ERG peak to peak amplitude in *tipE*^{1}*,se* mutants between temperature conditions, however, there was an evident trend towards decreased ERG amplitude at elevated temperature. Temperature sensitive paralytic mutants are known to increasingly lose the on/off transients from ERG traces with increasing temperature (Kelly & Suzuki, 1974). The trend seen in our *tipE*^{1}*,se* mutants suggests that they have a reversible decline in visual function at higher temperatures. Thus, the aberration is present throughout the nervous system rather than being confined to the motor neuronal system. The ERG recordings were more variable at elevated temperature, possibly because the flies became more agitated. Therefore, it could be advantageous to adapt the way in which the flies are restrained in the pipette tips during the ERG in an attempt to restrict their movement further. In addition, the number of responses recorded per ERG could be increased, for example from 5 to 20 responses, thus averaging out any potential movement during the ERG recording.

4.2. *Sepia* does not contribute to the temperature sensitive phenotype

The *tipE*^{1},se mutant strain has been kept for a number of decades. Due to the nature of some experiments, it could not be outcrossed to reduce the effects of

inbreeding, for example the incorporation of genetic modifiers (Kearney, 2011). An alternative way to test possible acquisition of genetic modifiers is by crossing the strain in question to a particular deficiency line. Deficiency lines carry a specific deletion which uncovers a gene of interest, creating a definitive null allele (Roote & Russell, 2012). When a mutant genotype is crossed to a deficiency line and the progeny display the known phenotype of the mutants, it can be inferred that the gene of interest has been uncovered by the deficiency, resulting in a hemizygous combination. An absence of the mutant phenotype in the progeny suggests the group of genes uncovered by the deficiency are not responsible for the phenotype. Various deficiency lines have been created to contain a heterozygous deletion within the same region as the gene of interest. This in turn reduces the dosage and uncovers the gene region.

Another advantage of crossing *tipE*^{1}*,se* mutant flies to a deficiency line was the ability to isolate the *sepia* gene. *tipE*^{1}*,se* mutants carry *tipE* (position 13.5) linked to *sepia* (position 27.0) on chromosome III (Kulkarni & Padhye, 1982; Feng *et al.*, 1995*b*). With the loci being in such close proximity to one another on the third chromosome, we wanted to ensure *tipE*^{1}*,se* mutant flies were exhibiting a temperature sensitive phenotype independent of the presence of *sepia*. This was in order to rule out any possibility that *sepia* was causing or contributing to the temperature sensitive phenotype. *tipE*^{1}*,se* mutant flies were crossed to the deficiency line $+;+;\frac{Df(3L)GN50}{TM8}$. We asked the question: are these flies temperature-sensitive paralytics and do they also exhibit a physiological deficit? The paralysis assay showed $+;+;\frac{tipE^{1},se}{Df(3L)GN50}$ to have a phenotype matching that of *tipE*^{1}*,se* flies. By creating a hemizygous combination that

uncovers the *tipE* locus, isolates *sepia* and consequently produces a temperature sensitive phenotype that mirrors that of *tipE[1],se* mutants, we conclude *sepia* is not the cause of the temperature-sensitive phenotype and that it is indeed as a result of the *tipE* mutation.

4.3. The *tipE[1],se* mutation likely results in a truncated protein rather than a protein null

The *tipE*[1],*se* mutation results in a premature STOP codon that could potentially truncate the *tipE* protein and relocate the intracellular C terminal region extracellularly (Feng *et al.*, 1995*a*). If possible regulatory sequences or interaction sites with other signalling partners are present in the C terminus, as is the case for β1 (Brackenbury & Isom, 2011), the *tipE[1]*,*se* mutation may disrupt such signalling giving rise to the observed locomotor phenotype.

Alternatively, the mutant mRNA transcript may be being degraded by nonsense-mediated decay, a eukaryotic surveillance pathway that reduces errors in gene expression by eliminating any mRNA transcripts containing premature STOP codons (Baker & Parker, 2004). On the other hand, if the tipE protein is present and truncated, it may function as a dominant negative, and inhibit function of the wild type gene product within the same cell (Herskowitz, 1987). One way to resolve these possibilities would be to perform a Western blot, however there is currently no commercially-available tipE antibody. Instead, RT-qPCR could be used to detect changes in the expression of *tipE* mRNA from both WT and *tipE[1],se* mutants. The lack of temperature-sensitive paralysis phenotype in a

heterozygote $\frac{w^-}{+}; +; \frac{tipE^1,se}{+}$ fly supports a loss-of-function model for the action of the *tipE*^{1}*,se* mutation.

The RNAi pathway in insects is very similar to that of other animals (Heigwer *et al.*, 2018). A biochemical pathway, it comes into play when exogenous dsRNA is introduced into the fly, in our case using the Valium10 vector, created as part of the TRiP project (Perkins *et al.*, 2015). This in turn leads to the formation of a complex consisting of dicer2, an enzyme responsible for cleaving dsRNA into shorter fragments, and R2D2, the dsRNA binding protein that binds dicer2 and loads siRNAs into the Argonaut protein (Ago2). As a result, Ago2 is induced, leading to the unwinding of dsRNA, its cleavage and subsequently ejection of the passenger strand. This as a whole is recognised as the RNA-induced silencer complex (RISC), which ultimately identifies sequence-homologous endogenous RNAs, leading to cleavage and degradation (Heigwer *et al.*, 2018).

tipE was knocked down by RNAi (without dicer2) globally, pan-neuronally, and in the motor neurons. Although not significantly different, there was a surprising trend towards an increased climbing ability in the RNAi lines. With *tipE*^{1},*se* mutants exhibiting a slight physiological deficit compared to wild type, it was expected that the RNAi lines would show a similar phenotype to that of *tipE*^{1},*se*. A further possible explanation for the disagreement in these data is that genetic compensation is occurring, in which levels of other proteins are being adjusted in response to, and to compensate for, the knockdown of *tipE*. It is possible that one of the four sequences homologous to *tipE*, TEH1-4 (Derst *et al.,* 2006), is compensating for the *tipE* knockdown, which may explain the phenotype seen.

The exact mechanism of genetic compensation is still poorly understood but it has been widely reported to have an effect in numerous model systems during gene knockdown studies (El-Brolosy & Stainier, 2017). An alternative possibility is that *tipE*-RNAi may be having off-target effects or is not efficient at knocking down the *tipE* transcript. The latter could be tested directly by RT-qPCR. We also did not test the possibility of *tipE* function in glia. Previously a *Drosophila* temperature sensitive mutation in the glial protein axotactin was seen to block action potentials at the non-permissive temperature (Yuan & Ganetzky, 1999). Future experiments could attempt RNAi knockdown of *tipE* in glia. In addition, several UAS and GAL4 driver lines were not used as controls due to time constraints (for example: $+;+;\frac{UAS-tipE-RNAi}{+}$, $+;\frac{Act5c-GAL4}{+};+$, $+;+;\frac{nSyb-GAL4}{+}$ and $+;\frac{OK6-GAL4}{+};+$).

By combining our RNAi line with dicer2 we aimed to increase the potency of our *tipE*-RNAi (Kim *et al.*, 2005). A climbing assay at room temperature indicated that *tipE* knockdown by RNAi and dicer2 in the muscle resulted in an increased climbing ability and hyperactivity at room temperature, suggesting that dicer2 did increase the potency of the RNAi and that loss of *tipE* confers an advantageous enhanced climbing phenotype. We knocked down *tipE* in the muscle primarily as a control for off target effects of RNAi however, additionally, we cannot assume that *tipE* only regulates *para,* which is not expressed in muscle (Derst *et al*., 2006; Suzuki *et al.*, 1971). For example, tipE may additionally regulate Slo channels present in the muscle (Derst *et al*., 2006). In contrast, elevated temperature had no effect on the dicer2-expressing RNAi lines. Together, these data suggest the need for a fine balance between *tipE* in

the muscles and in the nervous system in order to maintain physiological homeostasis. It has also been suggested that *tipE* and the four *tipE* homologous sequences TEH1-4 show similarity to Sloβ channels (Derst *et al*., 2006). Although *Para* sodium channels are lacking in *Drosophila* skeletal muscle, it has been shown that TEH2-4 may colocalise with *Drosophila* Sloβ channels, which are present within (and were first described in) muscle (Derst *et al*., 2006, Elkins *et al*., 1986). This could provide an explanation for the phenotype seen when attempting to knockdown *tipE* in the muscle. Further investigation is required to address this possibility and fully characterise these RNAi lines. Again, possible controls were not run due to time constraints (for example: $+; \frac{UAS-dicer2}{+}; \frac{nSyb-GAL4}{+}$ and $+; \frac{UAS-dicer2}{+}; \frac{MHC-GAL4}{+}$).

Although the efficiency of RNAi-mediated knock-down of the *tipE* transcript was not determined, the lack of a temperature sensitive phenotype in the RNAi stocks points towards the possibility that the *tipE^{1},se* mutation is resulting in a truncated protein, rather than a functional null due to nonsense-mediated decay. Further work would be required to evaluate the level of RNAi-mediated knock-down (e.g. by RT-qPCR) and confirm that the *tipE^{1},se* mutation does indeed produce a truncated protein.

4.4. Mammalian β1 mildly inhibits larval locomotor function

Our ultimate goal was to evaluate whether β1 expression in a *tipE* knockdown background could rescue the *tipE^{1},se* phenotype. Unfortunately, it was not possible to complete these crosses prior to thesis submission and so we undertook a preliminary experiment in which we tested the effect of expressing

mammalian β1 in the nervous system of a wild type fly. β1 expression had no effect on locomotor velocity. However, β1 expression did increase the number of turns at 25 °C. Given that the number of larval turns correlates with physiological stress (Günther *et al.*, 2016), this suggests that β1 expression may be having a mild detrimental effect on the larvae. The reasons for this are not clear. β1 is a CAM, with the adhesive functions being critical to brain development, neuronal excitability, neurite outgrowth, axon pathfinding and fasciculation (O'Malley & Isom, 2015). Given its multifunctionality, the expression of β1 could be having adverse effects on larval brain development. Fasciculation is a process that occurs during nervous system development in which growing axons interact, adhere together and form bundles (Bak & Fraser, 2003; Davis *et al.*, 2017). It is possible that β1 may not be interacting with *Drosophila* proteins but is adhering to other β1 subunits in adjacent neurons, causing aberrations in axon fasciculation or defasciculation that is ultimately resulting in the detrimental effect to larvae.

Although there is little sequence similarity between *tipE* and any mammalian VGSC subunit, functional expression of *para* Na^+ channels increases when *tipE* is expressed in *Xenopus laevis* oocytes (Feng *et al.*, 1995*a*). Analogously, co-expression of β subunits *in vitro* and *in vivo* leads to increased α subunit expression at the plasma membrane, which is thought to be due to β1-mediated trafficking of channels to the cell surface (McEwen *et al.*, 2004*b*; O'Malley & Isom, 2015). This indicates *tipE*, much like β1, supports the expression of VGSCs and modulates channel gating. Furthermore, *SCN1B* null mice have been found to exhibit ataxia, a phenotype that can be compared to the

physiological locomotor deficit seen in *tipE*^{1}*,se* mutant adults and larvae (Chen *et al.*, 2004). Further work should aim to establish the functional equivalence of *tipE* and β1 in regulating VGSC expression/activity.

4.5. Future directions

There are several avenues for future work based on the findings described in this thesis. Our research suggests that the *tipE*^{1}*,se* mutation is a loss of function mutation which is causing a neurological deficit, in addition to a temperature-sensitive phenotype. Moving forward, if we know a loss of function mutation is causing this deficit, we could investigate whether overexpressing wildtype *tipE* could improve physiological function. This can be done using the same technique used to express mammalian β1 in the flies, by fusing a *tipE* transgene to EGFP and cloning into the pUAST-AttB vector to be microinjected into fly embryos.

It is not currently known where *tipE* localises to within adult *Drosophila* neurons. Creating a fusion protein as described above will also allow localisation to be pinpointed using confocal microscopy at a cellular level, and a rescue experiment to be conducted, in which we would aim to rescue the temperature sensitive phenotype of *tipE*^{1}*,se* mutants with the *tipE-EGFP* transgene. In addition to this, we could also attempt a rescue using β1.

The results from the RNAi knockdown of *tipE* made it difficult to draw a solid conclusion without further exploration. The use of an additional driver, *tubulin-GAL4* which drives expression globally, could give us more of an insight. This was a cross we planned to set up during the project however, unfortunately, the

$+;\frac{UAS-dicer2}{CyO-GFP};\frac{tubulin-GAL4}{TM6b}$ stocks died and there was not enough time left to repeat the crosses. Additional controls, e.g. UAS and GAL4 driver lines, that were not included due to time constraints should also be run in order to address the possibility that differences are not as a result of genetic background. It will also be important to establish the effectiveness of the RNAi using RT-qPCR.

Western blot analysis would allow us to conclude whether or not the *tipE*^{1}*,se* mutation results in a truncated protein or a protein null. There is, however, no tipE antibody available, therefore this would need to be created first. In addition, further ERG analysis could be carried out to investigate ERG amplitude at both ambient and elevated temperatures using further genotypes used in this study, for example: $+;+;\frac{tipE^{1},se}{Df(3L)GN50}$ and any of the *tipE*-RNAi-dicer2 expressing stocks. Increasing the number of samples used in ERG experiments already carried out would also be beneficial and would hopefully produce a statistically significant result.

4.6. Conclusion

The work described in this thesis has uncovered new information on *tipE* and β1 function. In addition to a temperature-sensitive phenotype, we have uncovered a physiological deficit, which is exacerbated by an increase in temperature in both *Drosophila* adults and larvae. Moreover, our results provide evidence that the mutation may be causing this phenotype due to a protein truncation. The reversible decline in ERG amplitude at elevated temperature suggests the mutation causes an aberration throughout the nervous system rather than being confined to the motor neuronal system. However, further research is still

needed to determine whether or not *tipE* can serve as a functional orthologue to recapitulate some of the function of the VGSC β1 subunit.

References; in the style of The Journal of Physiology

Ahern CA, Payandeh J, Bosmans F & Chanda B (2016). The hitchhiker's guide to the voltage-gated sodium channel galaxy. *J Gen Physiol* **147,** 1–24.

Allaway D, Schofield NA, Leonard ME, Gilardoni L, Finan TM & Poole PS (2001). Use of differential fluorescence induction and optical trapping to isolate environmentally induced genes. *Environ Microbiol* **3,** 397–406.

Aoki T, Sugiura Y, Sugiyama Y, Ogata M, Hida C, Honma M & Yamamoto T (2000). [A family with heat-sensitive myotonia alternating with hypokalemic periodic paralysis]. *Rinsho Shinkeigaku* **40,** 358–363.

Aronica E, Troost D, Rozemuller AJ, Yankaya B, Jansen GH, Isom LL & Gorter JA (2003). Expression and regulation of voltage-gated sodium channel beta1 subunit protein in human gliosis-associated pathologies. *Acta Neuropathol* **105,** 515–523.

Atwood HL, Govind CK & Wu C-F (1993). Differential ultrastructure of synaptic terminals on ventral longitudinal abdominal muscles inDrosophila larvae. *J Neurobiol* **24,** 1008–1024.

Bagal SK, Marron BE, Owen RM, Storer RI & Swain NA (2015). Voltage gated sodium channels as drug discovery targets. *Channels (Austin)* **9,** 360–366.

Bak M & Fraser SE (2003). Axon fasciculation and differences in midline kinetics between pioneer and follower axons within commissural fascicles. *Development* **130,** 4999–5008.

Baker DA, Beckingham KM & Armstrong JD (2007). Functional dissection of the neural substrates for gravitaxic maze behavior inDrosophila melanogaster. *J Comp Neurol* **501,** 756–764.

Baker KE & Parker R (2004). Nonsense-mediated mRNA decay: terminating erroneous gene expression. *Curr Opin Cell Biol* **16,** 293–299.

Bischof J, Maeda RK, Hediger M, Karch F & Basler K (2007). An optimized transgenesis system for Drosophila using germ-line-specific phiC31 integrases. *Proc Natl Acad Sci U S A* **104,** 3312–3317.

Brackenbury WJ, Calhoun JD, Chen C, Miyazaki H, Nukina N, Oyama F, Ranscht B & Isom LL (2010). Functional reciprocity between Na+ channel Nav1.6 and 1 subunits in the coordinated regulation of excitability and neurite outgrowth. *Proc Natl Acad Sci* **107,** 2283–2288.

Brackenbury WJ, Davis TH, Chen C, Slat EA, Detrow MJ, Dickendesher TL, Ranscht B & Isom LL (2008). Voltage-Gated Na+ Channel 1 Subunit-Mediated Neurite Outgrowth Requires Fyn Kinase and Contributes to Postnatal CNS Development In Vivo. *J Neurosci* **28,** 3246–3256.

Brackenbury WJ & Isom LL (2011). Na Channel β Subunits: Overachievers of the Ion Channel Family. *Front Pharmacol* **2,** 53.

Brand H & Perrimon N (1993). *Targeted gene expression as a means of altering cell fates and generating dominant phenotypes*. Available at: http://dev.biologists.org/content/develop/118/2/401.full.pdf [Accessed October 2, 2018].

Bridges CB (1917). Deficiency. *Genetics* **2,** 445–465.

Cahoy JD, Emery B, Kaushal A, Foo LC, Zamanian JL, Christopherson KS, Xing Y, Lubischer JL, Krieg PA, Krupenko SA, Thompson WJ & Barres BA (2008). A Transcriptome Database for Astrocytes, Neurons, and Oligodendrocytes: A New Resource for Understanding Brain Development and Function. *J Neurosci* **28,** 264–278.

Cardona A, Saalfeld S, Tomancak P & Hartenstein V (2009). Drosophila brain development: closing the gap between a macroarchitectural and microarchitectural approach. *Cold Spring Harb Symp Quant Biol* **74,** 235–

248.

Chen C-L, Gajewski KM, Hamaratoglu F, Bossuyt W, Sansores-Garcia L, Tao C & Halder G (2010). The apical-basal cell polarity determinant Crumbs regulates Hippo signaling in Drosophila. *Proc Natl Acad Sci U S A* **107,** 15810–15815.

Chen C, Westenbroek RE, Xu X, Edwards CA, Sorenson DR, Chen Y, McEwen DP, O'Malley HA, Bharucha V, Meadows LS, Knudsen GA, Vilaythong A, Noebels JL, Saunders TL, Scheuer T, Shrager P, Catterall WA & Isom LL (2004). Mice Lacking Sodium Channel 1 Subunits Display Defects in Neuronal Excitability, Sodium Channel Expression, and Nodal Architecture. *J Neurosci* **24,** 4030–4042.

Chioni A-M, Brackenbury WJ, Calhoun JD, Isom LL & Djamgoz MBA (2009). A novel adhesion molecule in human breast cancer cells: voltage-gated Na+ channel beta1 subunit. *Int J Biochem Cell Biol* **41,** 1216–1227.

Crossley A, Crossley NA & Crossley C (1978). The morphology and development of the Drosophila muscular system. Available at: https://www.scienceopen.com/document?vid=492678c0-4a9a-46d6-bd5e-4da390c6d31d [Accessed November 27, 2018].

Davis O, Merrison-Hort R, Soffe SR & Borisyuk R (2017). Studying the role of axon fasciculation during development in a computational model of the Xenopus tadpole spinal cord. *Sci Rep* **7,** 13551.

Davis TH, Chen C & Isom LL (2004). Sodium Channel β1 Subunits Promote Neurite Outgrowth in Cerebellar Granule Neurons. *J Biol Chem* **279,** 51424–51432.

Derst C, Walther C, Veh RW, Wicher D & Heinemann SH (2006). Four novel sequences in Drosophila melanogaster homologous to the auxiliary para

sodium channel subunit TipE. *Biochem Biophys Res Commun* **339,** 939–948.

Diss JKJ, Fraser SP, Walker MM, Patel A, Latchman DS & Djamgoz MBA (2008). β-Subunits of voltage-gated sodium channels in human prostate cancer: quantitative in vitro and in vivo analyses of mRNA expression. *Prostate Cancer Prostatic Dis* **11,** 325–333.

Dong K, Du Y, Rinkevich F, Wang L & Xu P (2015). The Drosophila Sodium Channel 1 (DSC1): The founding member of a new family of voltage-gated cation channels. *Pestic Biochem Physiol* **120,** 36–39.

Duffy JB (2002). GAL4 system in Drosophila: A fly geneticist's Swiss army knife. *Genesis* **34,** 1–15.

Egri C & Ruben PC (2012). A hot topic. *Channels* **6,** 75–85.

Eijkelkamp N, Linley JE, Baker MD, Minett MS, Cregg R, Werdehausen R, Rugiero F & Wood JN (2012). Neurological perspectives on voltage-gated sodium channels. *Brain* **135,** 2585–2612.

El-Brolosy MA & Stainier DYR (2017). Genetic compensation: A phenomenon in search of mechanisms ed. Moens C. *PLOS Genet* **13,** e1006780.

Elkins T, Ganetzky B & Wu CF (1986). A Drosophila mutation that eliminates a calcium-dependent potassium current. *Proc Natl Acad Sci U S A* **83,** 8415.

Feng G, Deák P, Chopra M & Hall LM (1995*a*). Cloning and functional analysis of TipE, a novel membrane protein that enhances Drosophila para sodium channel function. *Cell* **82,** 1001–1011.

Feng G, Peter ", Kasbekar DP, Gilt94 DW & Hall LM (1995*b*). *Cytogenetic and Molecular Localization of ti$.d% A Gene Affecting Sodium Channels in Drosophila melanogastm*. Available at: http://repository.ias.ac.in/18316/1/308.pdf [Accessed December 3, 2018].

Frank CA, Wang X, Collins CA, Rodal AA, Yuan Q, Verstreken P & Dickman DK (2013). New approaches for studying synaptic development, function, and plasticity using Drosophila as a model system. *J Neurosci* **33,** 17560–17568.

Gaborit N, Le Bouter S, Szuts V, Varro A, Escande D, Nattel S & Demolombe S (2007). Regional and tissue specific transcript signatures of ion channel genes in the non-diseased human heart. *J Physiol* **582,** 675–693.

Gargano J, Martin I, Bhandari P & Grotewiel M (2005). Rapid iterative negative geotaxis (RING): a new method for assessing age-related locomotor decline in. *Exp Gerontol* **40,** 386–395.

Ghovanloo M-R, Abdelsayed M, Peters CH & Ruben PC (2018). A Mixed Periodic Paralysis & Myotonia Mutant, P1158S, Imparts pH-Sensitivity in Skeletal Muscle Voltage-gated Sodium Channels. *Sci Rep* **8,** 6304.

Gloor GB, Preston CR, Johnson-Schlitz DM, Nassif NA, Phillis RW, Benz WK, Robertson HM & Engels WR (1993). Type I repressors of P element mobility. *Genetics* **135,** 81–95.

Groth AC, Fish M, Nusse R & Calos MP (2004). Construction of transgenic Drosophila by using the site-specific integrase from phage phiC31. *Genetics* **166,** 1775–1782.

Günther MN, Nettesheim G & Shubeita GT (2016). Quantifying and predicting Drosophila larvae crawling phenotypes. *Sci Rep* **6,** 27972.

Heigwer F, Port F & Boutros M (2018). RNA Interference (RNAi) Screening in Drosophila. *Genetics* **208,** 853–874.

Herskowitz I (1987). Functional inactivation of genes by dominant negative mutations. *Nature* **329,** 219–222.

Hindle S, Afsari F, Stark M, Middleton CA, Evans GJO, Sweeney ST & Elliott

CJH (2013). Dopaminergic expression of the Parkinsonian gene LRRK2-G2019S leads to non-autonomous visual neurodegeneration, accelerated by increased neural demands for energy. *Hum Mol Genet* **22,** 2129–2140.

Hodges DD, Lee D, Preston CF, Boswell K, Hall LM & O'Dowd DK (2002). tipE regulates Na+-dependent repetitive firing in Drosophila neurons. *Mol Cell Neurosci* **19,** 402–416.

Hsu EJ, Zhu W, Schubert AR, Voelker T, Varga Z & Silva JR (2017). Regulation of Na+ channel inactivation by the DIII and DIV voltage-sensing domains. *J Gen Physiol* **149,** 389–403.

Ichinose H, Katoh S, Sueoka T, Titani K, Fujita K & Nagatsu T (1991). Cloning and sequencing of cDNA encoding human sepiapterin reductase--an enzyme involved in tetrahydrobiopterin biosynthesis. *Biochem Biophys Res Commun* **179,** 183–189.

Isom LL, De Jongh KS & Catterall WA (1994). Auxiliary subunits of voltage-gated ion channels. *Neuron* **12,** 1183–1194.

Isom LL, De Jongh KS, Patton DE, Reber BF, Offord J, Charbonneau H, Walsh K, Goldin AL & Catterall WA (1992). Primary structure and functional expression of the beta 1 subunit of the rat brain sodium channel. *Science* **256,** 839–842.

Isom LL, Ragsdale DS, De Jongh KS, Westenbroek RE, Reber BFX, Scheuer T & Catterall WA (1995). Structure and function of the β2 subunit of brain sodium channels, a transmembrane glycoprotein with a CAM motif. *Cell* **83,** 433–442.

Jennings BH (2011). Drosophila – a versatile model in biology & medicine. *Mater Today* **14,** 190–195.

Jurkat-Rott K & Lehmann-Horn F (2010). State of the art in hereditary muscle

channelopathies. *Acta Myol myopathies cardiomyopathies Off J Mediterr Soc Myol* **29,** 343–350.

Kaufmann SG, Westenbroek RE, Maass AH, Lange V, Renner A, Wischmeyer E, Bonz A, Muck J, Ertl G, Catterall WA, Scheuer T & Maier SKG (2013). Distribution and function of sodium channel subtypes in human atrial myocardium. *J Mol Cell Cardiol* **61,** 133–141.

Kearney JA (2011). Genetic modifiers of neurological disease. *Curr Opin Genet Dev* **21,** 349–353.

Kelly LE & Suzuki DT (1974). The effects of increased temperature on electroretinograms of temperature-sensitive paralysis mutants of Drosophila melanogaster. *Proc Natl Acad Sci U S A* **71,** 4906–4909.

Kim D-H, Behlke MA, Rose SD, Chang M-S, Choi S & Rossi JJ (2005). Synthetic dsRNA Dicer substrates enhance RNAi potency and efficacy. *Nat Biotechnol* **23,** 222–226.

Kim J, Suh H, Kim S, Kim K, Ahn C & Yim J (2006). Identification and characteristics of the structural gene for the Drosophila eye colour mutant sepia, encoding PDA synthase, a member of the omega class glutathione S-transferases. *Biochem J* **398,** 451–460.

Koh YH, Gramates LS & Budnik V (2000). Drosophila larval neuromuscular junction: Molecular components and mechanisms underlying synaptic plasticity. *Microsc Res Tech* **49,** 14–25.

Kremer MC, Jung C, Batelli S, Rubin GM & Gaul U (2017). The glia of the adult Drosophila nervous system. *Glia* **65,** 606–638.

Kroll JR, Saras A & Tanouye MA (2015). Drosophila sodium channel mutations: Contributions to seizure-susceptibility. *Exp Neurol* **274,** 80–87.

Kulkarni SJ & Padhye A (1982). Temperature-sensitive paralytic mutations on

the second and third chromosomes of Drosophila melanogaster. *Genet Res* **40,** 191–199.

Larsen C, Shy D, Spindler SR, Fung S, Pereanu W, Younossi-Hartenstein A & Hartenstein V (2009). Patterns of growth, axonal extension and axonal arborization of neuronal lineages in the developing Drosophila brain. *Dev Biol* **335,** 289–304.

Lin W-H, Wright DE, Muraro NI & Baines RA (2009). Alternative Splicing in the Voltage-Gated Sodium Channel DmNav Regulates Activation, Inactivation, and Persistent Current. *J Neurophysiol* **102,** 1994–2006.

Littleton JT & Ganetzky B (2000). Ion channels and synaptic organization: analysis of the Drosophila genome. *Neuron* **26,** 35–43.

Lopez-Santiago LF, Meadows LS, Ernst SJ, Chen C, Malhotra JD, McEwen DP, Speelman A, Noebels JL, Maier SKG, Lopatin AN & Isom LL (2007). Sodium channel Scn1b null mice exhibit prolonged QT and RR intervals. *J Mol Cell Cardiol* **43,** 636–647.

Lopez-Santiago LF, Pertin M, Morisod X, Chen C, Hong S, Wiley J, Decosterd I & Isom LL (2006). Sodium Channel 2 Subunits Regulate Tetrodotoxin-Sensitive Sodium Channels in Small Dorsal Root Ganglion Neurons and Modulate the Response to Pain. *J Neurosci* **26,** 7984–7994.

Maier SKG, Westenbroek RE, McCormick KA, Curtis R, Scheuer T & Catterall WA (2004). Distinct Subcellular Localization of Different Sodium Channel α and β Subunits in Single Ventricular Myocytes From Mouse Heart. *Circulation* **109,** 1421–1427.

Maier SKG, Westenbroek RE, Yamanushi TT, Dobrzynski H, Boyett MR, Catterall WA & Scheuer T (2003). An unexpected requirement for brain-type sodium channels for control of heart rate in the mouse sinoatrial node.

Proc Natl Acad Sci **100,** 3507–3512.

Malhotra JD, Kazen-Gillespie K, Hortsch M & Isom LL (2000). Sodium channel beta subunits mediate homophilic cell adhesion and recruit ankyrin to points of cell-cell contact. *J Biol Chem* **275,** 11383–11388.

McEwen DP, Meadows LS, Chen C, Thyagarajan V & Isom LL (2004*a*). Sodium Channel β1 Subunit-mediated Modulation of $Na_v1.2$ Currents and Cell Surface Density Is Dependent on Interactions with Contactin and Ankyrin. *J Biol Chem* **279,** 16044–16049.

McEwen DP, Meadows LS, Chen C, Thyagarajan V & Isom LL (2004*b*). Sodium Channel β1 Subunit-mediated Modulation of Nav1.2 Currents and Cell Surface Density Is Dependent on Interactions with Contactin and Ankyrin. *J Biol Chem* **279,** 16044–16049.

Naylor CE, Bagnéris C, DeCaen PG, Sula A, Scaglione A, Clapham DE & Wallace BA (2016). Molecular basis of ion permeability in a voltage-gated sodium channel. *EMBO J* **35,** 820–830.

Nériec N & Desplan C (2016). From the Eye to the Brain: Development of the Drosophila Visual System. *Curr Top Dev Biol* **116,** 247–271.

Nguyen HM, Miyazaki H, Hoshi N, Smith BJ, Nukina N, Goldin AL & Chandy KG (2012). Modulation of voltage-gated K+ channels by the sodium channel 1 subunit. *Proc Natl Acad Sci* **109,** 18577–18582.

Ni J-Q, Liu L-P, Binari R, Hardy R, Shim H-S, Cavallaro A, Booker M, Pfeiffer BD, Markstein M, Wang H, Villalta C, Laverty TR, Perkins LA & Perrimon N (2009). A Drosophila resource of transgenic RNAi lines for neurogenetics. *Genetics* **182,** 1089–1100.

O'Malley HA & Isom LL (2015). Sodium Channel β Subunits: Emerging Targets in Channelopathies. *Annu Rev Physiol* **77,** 481–504.

Oh Y, Lee YJ & Waxman SG (1997). Regulation of Na+ channel beta 1 and beta 2 subunit mRNA levels in cultured rat astrocytes. *Neurosci Lett* **234,** 107–110.

Oh Y, Sashihara S, Black JA & Waxman SG (1995). Na+ channel beta 1 subunit mRNA: differential expression in rat spinal sensory neurons. *Brain Res Mol Brain Res* **30,** 357–361.

Orio P, Rojas P, Ferreira G & Latorre R (2002). New Disguises for an Old Channel: MaxiK Channel β-Subunits. *Physiology* **17,** 156–161.

Pak WL (2010). Why Drosophila to study phototransduction? *J Neurogenet* **24,** 55–66.

Patel F & Brackenbury WJ (2015). Dual roles of voltage-gated sodium channels in development and cancer. *Int J Dev Biol* **59,** 357–366.

Peng H, Chung P, Long F, Qu L, Jenett A, Seeds AM, Myers EW & Simpson JH (2011). BrainAligner: 3D registration atlases of Drosophila brains. *Nat Methods* **8,** 493–500.

Perkins LA et al. (2015). The Transgenic RNAi Project at Harvard Medical School: Resources and Validation. *Genetics* **201,** 843–852.

Persson B, Kallberg Y, Bray JE, Bruford E, Dellaporta SL, Favia AD, Duarte RG, Jörnvall H, Kavanagh KL, Kedishvili N, Kisiela M, Maser E, Mindnich R, Orchard S, Penning TM, Thornton JM, Adamski J & Oppermann U (2009). The SDR (short-chain dehydrogenase/reductase and related enzymes) nomenclature initiative. *Chem Biol Interact* **178,** 94–98.

Pröbstle T, Rüdel R & Ruppersberg JP (1988). Hodgkin-Huxley parameters of the sodium channels in human myoballs. *Pflugers Arch* **412,** 264–269.

Prüßing K, Voigt A & Schulz JB (2013). Drosophila melanogaster as a model organism for Alzheimer's disease. *Mol Neurodegener* **8,** 35.

Ratcliffe CF, Westenbroek RE, Curtis R & Catterall WA (2001). Sodium channel beta1 and beta3 subunits associate with neurofascin through their extracellular immunoglobulin-like domain. *J Cell Biol* **154,** 427–434.

Rinkevich FD, Du Y, Tolinski J, Ueda A, Wu C-F, Zhorov BS & Dong K (2015). Distinct roles of the DmNav and DSC1 channels in the action of DDT and pyrethroids. *Neurotoxicology* **47,** 99–106.

Roger S, Gillet L, Le Guennec J-Y & Besson P (2015). Voltage-gated sodium channels and cancer: is excitability their primary role? *Front Pharmacol* **6,** 152.

Roote J & Russell S (2012). Toward a complete Drosophila deficiency kit. *Genome Biol* **13,** 149.

Ruff RL (1999). Effects of temperature on slow and fast inactivation of rat skeletal muscle Na^+ channels. *Am J Physiol Physiol* **277,** C937–C947.

Ryder E et al. (2007). The DrosDel deletion collection: a Drosophila genomewide chromosomal deficiency resource. *Genetics* **177,** 615–629.

Sato M, Suzuki T & Nakai Y (2013). Waves of differentiation in the fly visual system. *Dev Biol* **380,** 1–11.

Siddiqi O & Benzer S (1976). Neurophysiological defects in temperature-sensitive paralytic mutants of Drosophila melanogaster. *Proc Natl Acad Sci U S A* **73,** 3253–3257.

Spindler SR & Hartenstein V (2010). The Drosophila neural lineages: a model system to study brain development and circuitry. *Dev Genes Evol* **220,** 1–10.

Sugiura Y, Aoki T, Sugiyama Y, Hida C, Ogata M & Yamamoto T (2000). Temperature-sensitive sodium channelopathy with heat-induced myotonia and cold-induced paralysis. *Neurology* **54,** 2179–2181.

Suzuki DT, Grigliatti T & Williamson R (1971). Temperature-sensitive mutations in Drosophila melanogaster. VII. A mutation (para-ts) causing reversible adult paralysis. *Proc Natl Acad Sci U S A* **68,** 890–893.

Thomas EA, Hawkins RJ, Richards KL, Xu R, Gazina E V. & Petrou S (2009). Heat opens axon initial segment sodium channels: A febrile seizure mechanism? *Ann Neurol* **66,** 219–226.

Vilinsky I & Johnson KG (2012). Electroretinograms in Drosophila: A Robust and Genetically Accessible Electrophysiological System for the Undergraduate Laboratory. *J Undergrad Neurosci Educ* **11,** A149.

Wallace RH, Wang DW, Singh R, Scheffer IE, George AL, Phillips HA, Saar K, Reis A, Johnson EW, Sutherland GR, Berkovic SF & Mulley JC (1998). Febrile seizures and generalized epilepsy associated with a mutation in the Na+-channel ß1 subunit gene SCN1B. *Nat Genet* **19,** 366–370.

Wang L, Nomura Y, Du Y & Dong K (2013). Differential Effects of TipE and a TipE-Homologous Protein on Modulation of Gating Properties of Sodium Channels from Drosophila melanogaster. *PLoS One*; DOI: 10.1371/journal.pone.0067551.

Warmke JW, Reenan RA, Wang P, Qian S, Arena JP, Wang J, Wunderler D, Liu K, Kaczorowski GJ, Van der Ploeg LH, Ganetzky B & Cohen CJ (1997). Functional expression of Drosophila para sodium channels. Modulation by the membrane protein TipE and toxin pharmacology. *J Gen Physiol* **110,** 119–133.

Watanabe H, Koopmann TT, Le Scouarnec S, Yang T, Ingram CR, Schott J-J, Demolombe S, Probst V, Anselme F, Escande D, Wiesfeld ACP, Pfeufer A, Kääb S, Wichmann H-E, Hasdemir C, Aizawa Y, Wilde AAM, Roden DM & Bezzina CR (2008). Sodium channel β1 subunit mutations associated with

Brugada syndrome and cardiac conduction disease in humans. *J Clin Invest* **118,** 2260–2268.

West RJH, Furmston R, Williams CAC & Elliott CJH (2015*a*). Neurophysiology of Drosophila models of Parkinson's disease. *Parkinsons Dis* **2015,** 381281.

West RJH, Lu Y, Marie B, Gao F-B & Sweeney ST (2015*b*). Rab8, POSH, and TAK1 regulate synaptic growth in a *Drosophila* model of frontotemporal dementia. *J Cell Biol* **208,** 931–947.

Wiederrecht GJ, Paton DR & Brown GM (1984). Enzymatic conversion of dihydroneopterin triphosphate to the pyrimidodiazepine intermediate involved in the biosynthesis of the drosopterins in Drosophila melanogaster. *J Biol Chem* **259,** 2195–2200.

Wolf MJ & Rockman HA (2008). Drosophila melanogaster as a model system for genetics of postnatal cardiac function. *Drug Discov Today Dis Models* **5,** 117–123.

Yim J, Kim K & Kim H (2015). Functional analysis of sepiapterin reductase in Drosophila melanogaster. *Pteridines* **26,** 63–68.

Yu FH, Westenbroek RE, Silos-Santiago I, McCormick KA, Lawson D, Ge P, Ferriera H, Lilly J, DiStefano PS, Catterall WA, Scheuer T, Curtis R, Noebels JL, Saunders TL, Scheuer T, Shrager P, Catterall WA & Isom LL (2003). Sodium channel beta4, a new disulfide-linked auxiliary subunit with similarity to beta2. *J Neurosci* **23,** 7577–7585.

Yuan LL & Ganetzky B (1999). A glial-neuronal signaling pathway revealed by mutations in a neurexin-related protein. *Science* **283,** 1343–1345.

Zhang T, Wang Z, Wang L, Luo N, Jiang L, Liu Z, Wu C-F & Dong K (2013). Role of the DSC1 Channel in Regulating Neuronal Excitability in Drosophila

melanogaster: Extending Nervous System Stability under Stress ed. Anholt RRH. *PLoS Genet* **9,** e1003327.

Zhao J, O'Leary ME & Chahine M (2011). Regulation of Na_v 1.6 and Na_v 1.8 peripheral nerve Na^+ channels by auxiliary β-subunits. *J Neurophysiol* **106,** 608–619.

Zhu Y (2013). The Drosophila visual system: From neural circuits to behavior. *Cell Adh Migr* **7,** 333–344.